COO-4131-T1(Vol.10)
Distribution Category UC-60

VOLUME X

WIND ENERGY CONVERSION

ASRL TR-184-16

AEROELASTIC STABILITY OF WIND TURBINE ROTOR BLADES

J. Wendell

Aeroelastic and Structures Research Laboratory

Department of Aeronautics and Astronautics

Massachusetts Institute of Technology

PREPARED FOR

U.S. DEPARTMENT OF ENERGY

UNDER CONTRACT NO. E(11.1)-4131

September 1978

DISCLAIMER

AEROELASTIC STABILITY OF WIND TURBINE ROTOR BLADES

ABSTRACT

The nonlinear equations of motion of a general wind turbine rotor blade are derived from first principles. The twisted, tapered blade may be preconed out of the plane of rotation, and its root may be offset from the axis of rotation by a small amount. The aerodynamic center, center of mass, shear center, and area centroid are distinct in this derivation. The equations are applicable to studies of forced response or of aeroelastic flutter, however, neither gravity forcing, nor wind shear and gust forcing are included.

The equations derived are applied to study the aeroelastic stability of the NASA-ERDA 100 kw wind turbine, and solved using the Galerkin method. The numerical results are used in conjunction with a mathematical comparison to prove the validity of an equivalent hinge model developed by the Wind Energy Conversion Project at the Massachusetts Institute of Technology.

TABLE OF CONTENTS

TABLE OF CONTENTS Continued

TABLE OF CONTENTS Continued

NOMENCLATURE

XYZ	Rotation coordinates with unit vectors $\hat{I}\hat{J}\hat{K}$
xyz	Blade coordinates with unit vectors $\hat{i}\hat{j}\hat{k}$
$x_2y_2z_2$	Airfoil coordinates with unit vectors $\hat{i}_2\hat{j}_2\hat{k}_2$
$\xi\eta\zeta$	Cross-section coordinates with unit vectors $\hat{i}_\xi\hat{i}_\eta\hat{i}_\zeta$
a	Airfoil liftcurve slope
$\hat{a}$	Absolute acceleration
c	Blade chord
d	Distributed aerodynamic drag
e_A	Aerodynamic center offset forward of the elastic axis
e_I	Center of mass offset forward of the elastic axis
e_T	Area centroid offset forward of the elastic axis
e_X	Blade root offset along X
e_Y	Blade root offset along Y
$\dot{h}$	Airfoil perpendicular oscillation
k_Δ	Radius of gyration of cross-section area
k_m	Radius of gyration of cross-section mass
ℓ_{nc}, ℓ_c	Distributed aerodynamic lift
m_{EA}	Distributed aerodynamic moment about the elastic axis.
m	Blade mass per unit length
$\hat{n}$	Normal unit vector

NOMENCLATURE Continued

$\mathring{p}$	Airstream pulsation
p_i	Distributed forces
ζ_i	Distributed moments
$\zeta_v, \zeta_w, \zeta_\phi$	Generalized coordinates
$\hat{r}_e$	Root offset vector
$\hat{r}_{db}$	Deformed blade radius vector
$\hat{r}_c$	Cross-section radius vector
t	Time
$\hat{t}$	Tangent unit vector
u_{inflow}	Induced inflow velocity of the air through the rotor disk
u	Deformation along x
v	Deformation along y
w	Deformation along z
C_{D_0}	Airfoil profile drag coefficient
$C(k)$	Lift deficiency function
$\underset{\sim}{C}$	Damping matrix
E	Young's modulus
EA,EI,EB	Blade cross-section integrals
GJ	Torsional stiffness
I_B	Mass moment of inertia of blade about root
$\underset{\sim}{K}$	Stiffness matrix
K_R	Pitch control system stiffness

NOMENCLATURE Continued

L	Blade length
$\underset{\sim}{M}$	Mass matrix
M_i	Moment stress resultant
$\underset{\sim}{P}$	Non-linear stiffness matrix
$\underset{\sim}{Q}$	Steady loads matrix
Q	Torque stress resultant
$\vec{R}$	Radius vector from axis of rotation
R_T	Blade tip radius
T	Tension stress resultant
V_i	Transverse shear
α	Airfoil steady angle of attack
β_p	Precone angle
$\beta_E, \phi_E, \theta_E$	Equivalent hinge coordinates
$\bar{\gamma}$	Locke number, modified
$\gamma_v, \gamma_w, \gamma_\phi$	Mode shapes, first natural mode
$\omega_v, \omega_w, \omega_\phi$	First natural frequencies
θ	Blade built in twist
θ_i	Airfoil incidence angle
ϕ	Twisting deformation about x
ε	Blade fiber strain
σ	Blade fiber stress
λ	Induced inflow angle
Ω	Blade rotation speed

NOMENCLATURE Continued

$\bar{\omega}$	Blade angular velocity
ψ	Azimuth angle of blade about z
ρ	Air density
ρ_b	Blade material density

Special Notation:

$(\,)'$	$\frac{\partial}{\partial x}$ in Part A, $\frac{\partial}{\partial \bar{x}}$ in Part B
$(\dot{})$	$\frac{\partial}{\partial t}$
$(\,)^{\circ}$	$\frac{\partial}{\partial \psi}$
$(\bar{})$	Non-dimensional quantity
$(\tilde{})$	Perturbation quantity
$(\,)_s$	Static quantity
$(\underset{\sim}{})$	Matrix
$(\,)^I$	Inertial
$(\,)^A$	Aerodynamic
$(\,)_{x,y,etc.}$	Vector components

Chapter I

INTRODUCTION

Wind turbines have enjoyed increased interest in recent years as a source of untapped energy.[1-4] This current resurgence has been fuelled mostly by the so called energy crisis, but wind power is by no means a new idea; the wind is an ancient source of power for ships, pumping water, grinding grain. Large wind turbines as sources of power became a popular idea in the early 1900's, especially in Europe, only to be quickly forgotten in the shadow of cheaper fossil fuel sources.[2]

In the United States, one early effort was the Putnam wind turbine,[3] which operated on Grandpa's Knob in Vermont from 1941 to 1945, supplying electric power to the Central Vermont Public Service Corporation. More recently, NASA and ERDA have erected large wind turbines in Sandusky, Ohio and Clayton, New Mexico.[4-6] Unlike the privately financed Putnam turbine, these are government sponsored experimental wind turbines.

Modern wind turbines are characterized by high rotational speeds and have attendant problems of material fatigue of the blades due to aerodynamic and gravity forcing, as well as aeroelastic flutter. The fact that the Putnam wind turbine program ended after a fatigue failure of a

blade illustrates the importance of understanding blade dynamics. Large amplitude forced response of the blades may reduce their expected life, driving the cost of the system up; aeroelastic flutter might result in catastropic failure.

Part A of this thesis concerns the derivation of the basic equations of motion of a general wind turbine blade using a Newtonian approach. From the outset, it must be realized that the behavior of this system is highly non-linear. Throughout the derivation, only the most important non-linear terms are retained. This process is implicit at each step.

Many published works in the area of rotary-wing dynamics derive similar equations, but sometimes steps are left out. Since the derivation is important to the understanding of the aeroelastic phenomenon and of the limitations of the final equations, it is included here, step by step, beginning from basic principles. Nonetheless, the uninterested reader may want to skip the very algebraic Chapters IV, V, and VI.

These equations of motion are the jump-off point for the study of forced response and aeroelastic flutter of wind turbine blades. Part B of this work is an Aeroelastic Stability Study of the NASA-ERDA 100 kw wind turbine (MOD-0), demonstrating a simple assumed-mode solution technique. An important facet of the method employed is the

linearization of the non-linear equations about a static deflected blade position, as opposed to linearization about the blade initial position. This is very important due to the dominance of inertia loads, which are very sensitive to blade displacement.

Another driving force for this work has been the need to verify calculations made using an "equivalent hinge" model developed for the Wind Energy Conversion Project at the Massachusetts Institute of Technology.[1] This model was used to generate aeroelastic stability plots for an extensive parametric variation.

To keep the text clear and concise, coordinate transformation, as well as all numerical data and calculations, have been relegated to the Appendices.

PART A

DERIVATION OF EQUATIONS OF MOTION

Chapter II

Coordinate Systems and Transformations

The choice of coordinate axes is very important to the derivation of the equations of motion, both for understanding and for convenience. This will be evident later.

2.1 General Coordinates

Figure 2.1 shows the coordinate systems to be used. The blade axis system (cartesian, xyz) has its origin at the blade root, which may be hinged or cantilevered. The x axis is the locus of the cross-section shear centers, which is assumed to be straight. The y axis is in the plane of rotation defined by X and Y, and parallel to Y, however the x axis may be coned out of the plane of rotation by the angle β_p. The root of the blade is offset from the XYZ origin by the amounts e_X and e_Y as shown. Z defines the axis of rotation, and both xyz and XYZ rotate together about Z with angular velocity Ω. Unit vectors in the xyz and XYZ systems are $\hat{i}\hat{j}\hat{k}$ and $\hat{I}\hat{J}\hat{K}$, respectively.

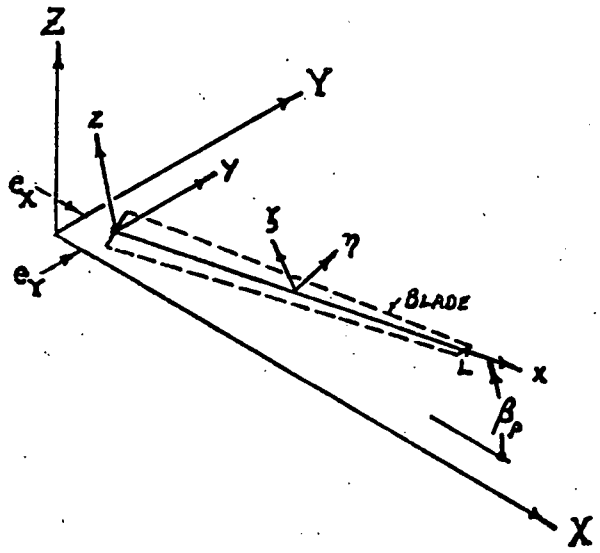

Fig. 2.1

2.2 Cross-section Coordinates and Deformations

Coordinates ξ, η, and ζ locate points within the blade cross section as shown by Fig. 2.2. η is parallel to the wing section chord and ζ is perpendicular to it, with the origin at the section shear center. ξ is an auxiliary coordinate along x. η and ζ are rotated an angle $\theta(x)$ from y and z.

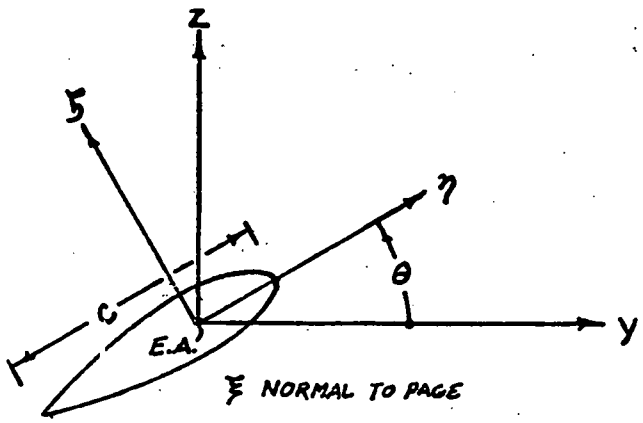

Fig. 2.2

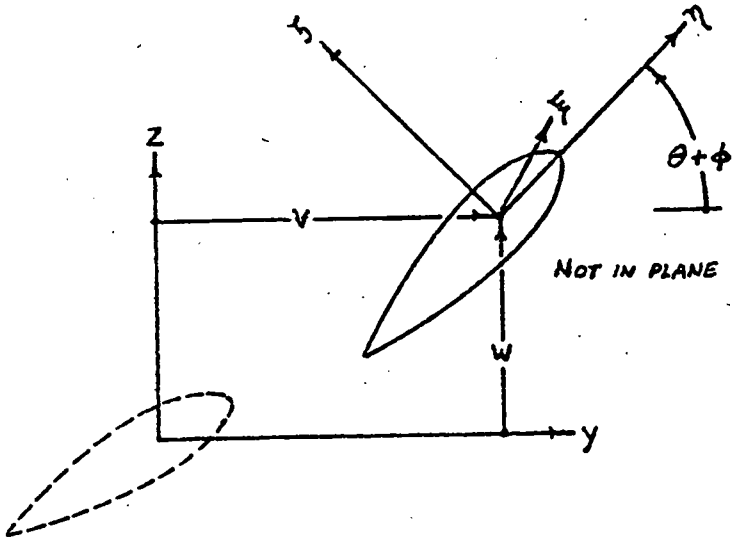

Fig. 2.3

The blade deforms away from the xyz coordinate system as shown by Fig. 2.3. In the x direction, a point of the blade moves an amount u; in the y direction, an amount v; and in the z direction, an amount w. Further, the blade rotates about x an angle ϕ so that the total angle from y and z to η and ζ is now $\theta + \phi$. The unit vectors in the ξ, η and ζ directions are $\hat{i}_\xi$, $\hat{i}_\eta$, $\hat{i}_\zeta$.

2.3 Coordinate Transformations

The XYZ, xyz, and $\xi\eta\zeta$ systems can be related by transformation matrices as follows:

$$\begin{Bmatrix} \hat{I} \\ \hat{J} \\ \hat{K} \end{Bmatrix} = \begin{bmatrix} \cos\beta_p & 0 & -\sin\beta_p \\ 0 & 1 & 0 \\ \sin\beta_p & 0 & \cos\beta_p \end{bmatrix} \begin{Bmatrix} \hat{i} \\ \hat{j} \\ \hat{k} \end{Bmatrix} \qquad (2.1)$$

$$\begin{Bmatrix} \hat{\imath}_\xi \\ \hat{\imath}_\eta \\ \hat{\imath}_\zeta \end{Bmatrix} = \begin{bmatrix} (1-\frac{1}{2}v'^2-\frac{1}{2}w'^2) & v' & w' \\ -(v'\cos(\theta+\phi)+w'\sin(\theta+\phi)) & \cos(\theta+\phi) & \sin(\theta+\phi) \\ -(w'\cos(\theta+\phi)-v'\sin(\theta+\phi)) & -\sin(\theta+\phi) & \cos(\theta+\phi) \end{bmatrix} \begin{Bmatrix} \hat{\imath} \\ \hat{\jmath} \\ \hat{k} \end{Bmatrix} \qquad (2.2)$$

where: $(\quad)' = \frac{\partial}{\partial x}$

2.4 Radius Vector

The radius vector to any point on the deformed blade may be conveniently broken up into three parts (Fig. 2.4):

$$\vec{R} = \vec{r}_e + \vec{r}_{db} + \vec{r}_c \qquad (2.3)$$

where:

$$\vec{r}_e = \begin{bmatrix} e_x & e_y & 0 \end{bmatrix} \begin{Bmatrix} \hat{I} \\ \hat{J} \\ \hat{K} \end{Bmatrix}$$

$$\vec{r}_{db} = \begin{bmatrix} (x+u) & v & w \end{bmatrix} \begin{Bmatrix} \hat{\imath} \\ \hat{\jmath} \\ \hat{k} \end{Bmatrix}$$

$$\vec{r}_c = \begin{bmatrix} 0 & \eta & \zeta \end{bmatrix} \begin{Bmatrix} \hat{\imath}_\xi \\ \hat{\imath}_\eta \\ \hat{\imath}_\zeta \end{Bmatrix}$$

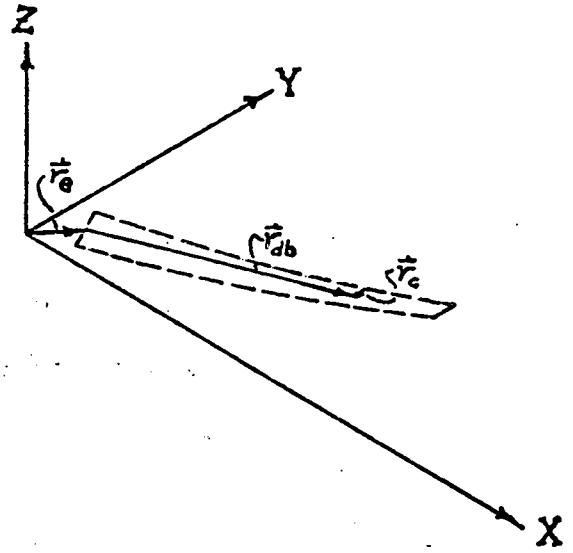

Fig. 2.4

The components of these vectors are now transformed into the xyz system and the vectors added to yield:

$$\vec{R} = \begin{Bmatrix} x + e_x \cos\beta_p + u - \eta(v'\cos(\theta+\phi)+w'\sin(\theta+\phi)) \\ \qquad -\zeta(w'\cos(\theta+\phi)-v'\sin(\theta+\phi)) \\ e_Y + V + \eta\cos(\theta+\phi) - \zeta\sin(\theta+\phi) \\ -e_x \sin\beta_p + W + \eta\sin(\theta+\phi) + \zeta\cos(\theta+\phi) \end{Bmatrix}^T \begin{Bmatrix} \hat{i} \\ \hat{j} \\ \hat{k} \end{Bmatrix} \qquad (2.4)$$

Chapter III

Ordering Scheme

In the following derivations, many higher order terms will be generated. Only the largest and most important ones will be kept, to keep the equations as simple as possible.

To facilitate this sorting of terms, an ordering scheme is established here which assigns approximate relative orders of magnitude to all the variables and parameters involved.

All of the orders of magnitude are refered to the magnitude of the bending slopes, v' and w', which are given a value ϵ_0. Table 3.1 lists the variables and parameters and assumed magnitudes. Some of these have not been used as yet but are defined briefly in the nonmenclature list.

$O(\epsilon_0^2)$: $\frac{e_{30}}{a}$, $\frac{u}{L}$, u'

$O(\epsilon_0)$: v', w', ϕ, $\frac{v}{L}$, $\frac{w}{L}$, θ', α

$\bar{c}$, $\bar{e}_A$, $\bar{e}_I$, $\bar{e}_T$, $\bar{e}_X$, $\bar{e}_Y$, $\bar{k}_m$, $\bar{k}_A$

$O(\epsilon_0^{\frac{1}{2}})$: λ , β_p

$O(1)$: $\frac{x}{L}$, θ ; $\frac{\partial}{\partial x} = (\,)'$; $\frac{1}{\Omega}\frac{\partial}{\partial t} = \frac{1}{\Omega}(\dot{})$

Table 3.1

This ordering scheme may be compared to that used by Hodges and Dowell[7,8] or Friedmann,[9] for similar equations intended primarily for rotorcraft blades. Note that three parameters often regarded as small are not assumed so in this work:

1) Induced inflow angle, λ

2) Coning angle, β_p

3) Built-in pitch angle, θ

The small angle assumption is not used for these angles, because they may be considerably larger for wind turbines, as seen in Part B.

The ordering scheme is applied as follows: If an expression or grouping contains terms of 3 or more orders, for example $O(1 + \varepsilon_0 + \varepsilon_0^2 + \varepsilon_0^3)$ or $O(\varepsilon_0^3 + \varepsilon_0^4 + \varepsilon_0^5)$, only the largest two terms are kept. These examples then become $O(1 + \varepsilon_0)$ and $O(\varepsilon_0^3 + \varepsilon_0^4)$, respectively. This scheme is applied at each intermediate step to manage the size of the equations but retain the important terms. In some special cases the rule is relaxed, as noted later.

Finally, in any application of the equations derived, care must be taken to compare these assumed orders of magnitude to reality. The maximum values of all parameters, and the tip deflections indicated by the solution should be checked.

Chapter IV

Structural Equations

This chapter explains the derivation of the structural equations in some detail. The non-linear derivation follows closely the classic linear treatment of Houbolt and Brooks.[10]

4.1 Strain-Displacement Relations

The blade is assumed to be a slender beam, so that the only important strain acts along longitudinal fibers of the blade. Normal and shear strains are ignored, except that St. Venant torsion is superimposed in these equations at the proper juncture. The fiber strain ϵ is related to the arc length, ds in undeformed space, and dS in deformed space, by the simple quotient:

$$\epsilon = \frac{dS - ds}{ds} \tag{4.1}$$

The radius vector to any point on the deformed blade was given in Chapter II as:

$$\vec{R} = \begin{Bmatrix} x + e_x \cos\beta_p + u - \eta(v'\cos(\theta+\phi) + w'\sin(\theta+\phi)) \\ \qquad - \zeta(w'\cos(\theta+\phi) - v'\sin(\theta+\phi)) \\ e_y + v + \eta\cos(\theta+\phi) - \zeta\sin(\theta+\phi) \\ -e_x \sin\beta_p + w + \eta\sin(\theta+\phi) + \zeta\cos(\theta+\phi) \end{Bmatrix}^T \begin{Bmatrix} \hat{i} \\ \hat{j} \\ \hat{k} \end{Bmatrix} \tag{4.2}$$

Differentiating with respect to x yields:

$$\frac{d\vec{R}}{dx} = \begin{Bmatrix} 1+u' - \eta[(v''+w'(\theta+\phi)')\cos(\theta+\phi)+(w''-v'(\theta+\phi)')\sin(\theta+\phi)] \\ \quad -\zeta[(w''-v'(\theta+\phi)')\cos(\theta+\phi)-(v''+w'(\theta+\phi)')\sin(\theta+\phi)] \\ v' - \eta(\theta+\phi)'\sin(\theta+\phi) - \zeta(\theta+\phi)'\cos(\theta+\phi) \\ w' + \eta(\theta+\phi)'\cos(\theta+\phi) - \zeta(\theta+\phi)'\sin(\theta+\phi) \end{Bmatrix} \begin{Bmatrix} \hat{i} \\ \hat{j} \\ \hat{k} \end{Bmatrix} \quad (4.3)$$

The magnitude of this vector is $\frac{ds}{dx}$, which is calculated using the approximation $\sqrt{1+\varepsilon_0} \cong 1 + 1/2\ \varepsilon_0$. Discarding higher order terms gives:

$$\frac{dS}{dx} = 1 + u' + \frac{1}{2}v'^2 + \frac{1}{2}w'^2 + \frac{1}{2}(\eta^2+\zeta^2)(\theta'+\phi')^2 - \eta(v''\cos(\theta+\phi)+w''\sin(\theta+\phi)) - \zeta(w''\cos(\theta+\phi)-v''\sin(\theta+\phi)) \quad (4.4)$$

The original arc length is formed by setting $u = v = w = \phi = 0$, so that $u' = v' = w' = \phi' = v'' = w'' = 0$:

$$\frac{ds}{dx} = 1 + \frac{1}{2}(\eta^2+\zeta^2)\theta'^2 \quad (4.5)$$

Then:

$$\epsilon = \frac{\frac{dS}{dx} - \frac{ds}{dx}}{\frac{ds}{dx}} =$$

$$u' + \frac{1}{2}v'^2 + \frac{1}{2}w'^2 + (\eta^2+\zeta^2)(\theta'\phi' + \frac{1}{2}\phi'^2) - \eta(v''\cos(\theta+\phi)+w''\sin(\theta+\phi)) - \zeta(w''\cos(\theta+\phi)-v''\sin(\theta+\phi)) \quad (4.6)$$

where:

$$1/\frac{ds}{dx} \cong 1$$

4.2 Stress-Strain Relation and Blade Tension

The stress-strain relation is simply:

$$\sigma = E\epsilon \tag{4.7}$$

The blade tension is given by:

$$T = \underset{\text{cross-section}}{\iint} \sigma \, d\eta \, d\zeta = \iint E\epsilon \, d\eta \, d\zeta \tag{4.8}$$

Integration yields:

$$T = EA\left[u' + \tfrac{1}{2}v'^2 + \tfrac{1}{2}w'^2 + k_A^2(\theta'\phi' + \tfrac{1}{2}\phi'^2) - e_T(v''\cos(\theta+\phi) + w''\sin(\theta+\phi))\right] \tag{4.9}$$

$$EA = \underset{\text{cross-sect.}}{\iint} E \, d\eta \, d\zeta$$

$$e_T = \frac{1}{EA} \underset{\text{cross-sect.}}{\iint} E\eta \, d\eta \, d\zeta$$

$$k_A^2 = \frac{1}{EA} \iint E(\eta^2 + \zeta^2) \, d\eta \, d\zeta$$

$$\iint E\zeta \, d\eta \, d\zeta = 0 \qquad \text{ASSUME SYMMETRIC CROSS-SECTION.}$$

This expression is used to eliminate the terms $u' + \frac{1}{2}(v')^2 + \frac{1}{2}(w')^2$ from Eq. (4.6):

$$\epsilon = \frac{T}{EA} + (\eta^2 + \zeta^2 - k_A^2)(\theta'\phi' + \frac{1}{2}\phi'^2)$$
$$-(\eta - e_T)(v''\cos(\theta+\phi) + w''\sin(\theta+\phi))$$
$$-\zeta(w''\cos(\theta+\phi) - v''\sin(\theta+\phi)) \qquad (4.10)$$

Also:

$$\sigma = E\frac{T}{EA} + E(\eta^2 + \zeta^2 - k_A^2)(\theta'\phi' + \frac{1}{2}\phi'^2)$$
$$-E(\eta - e_T)(v''\cos(\theta+\phi) + w''\sin(\theta+\phi)) \qquad (4.11)$$
$$-E\,\zeta(w''\cos(\theta+\phi) - v''\sin(\theta+\phi))$$

4.3 Stress Resultants

The stresses in the blade are integrated over the cross-section to give the resultant moments (Fig. 4.1). A consistent right hand rule is used to calculate the moments about η and ζ:

$$M_\eta = \iint_{\text{cross-sect.}} \sigma\zeta\, d\eta\, d\zeta \qquad (4.12)$$

$$M_\zeta = -\iint_{\text{cross-sect.}} \sigma\eta\, d\eta\, d\zeta \qquad (4.13)$$

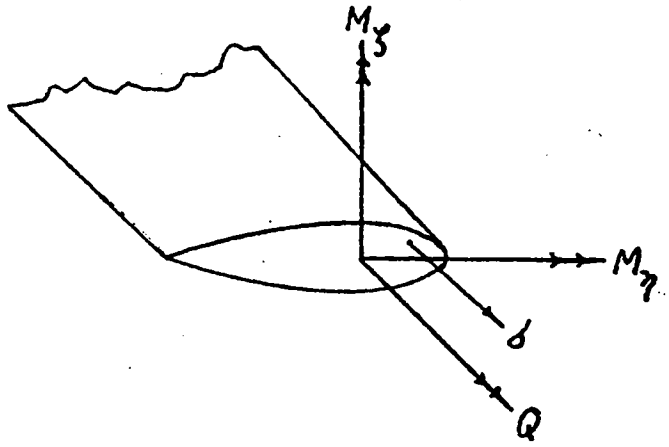

Fig. 4.1

The torque about ξ must be formulated with some care. Here, note the importance of the choice of x axis. The fact that it is the shear center means that the bending shears have no net moment about ξ. There is, however, a St. Venant torsion term which is added in.[10]

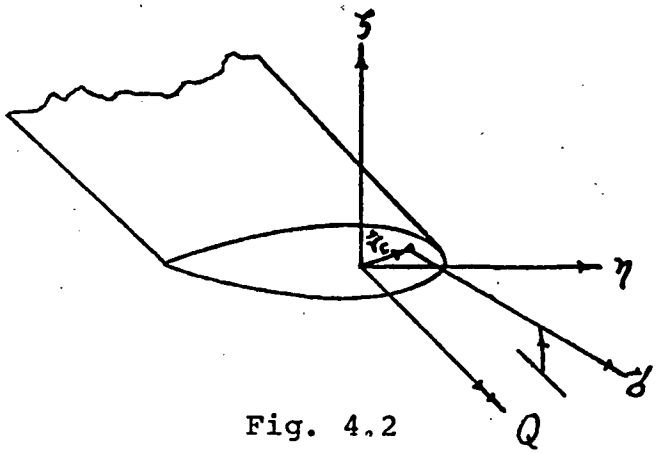

Fig. 4.2

Figure 4.2 shows the stress at an arbitrary point (η,ζ) in the cross-section. The stress vector makes a

slight angle to the ξ direction due to the finite twist rate of the blade, $(\theta + \phi)'$. Thus, a small moment results from the component of stress parallel to the cross-section. The distance from the stress vector to the shear center is $\sqrt{\eta^2 + \zeta^2}$; the angle can be shown to be approximately $(\theta + \phi)'\sqrt{\eta^2 + \zeta^2}$. Finally the torque is given by this small component, integrated over the cross-section, added to the classic St. Venant term:

$$Q = GJ\phi' + \iint_{\text{cross-sect.}} \sigma\,(\theta+\phi)'(\eta^2+\zeta^2)\,d\eta\,d\zeta \qquad (4.14)$$

Applying Eq. (4.11) to Eq. (4.12), (4.13) and (4.14), and integrating:

$$M_\eta = EI_\zeta\,[w''\cos(\theta+\phi) - v''\sin(\theta+\phi)]$$

$$M_\zeta = EI_\eta\,[v''\cos(\theta+\phi) + w''\sin(\theta+\phi)] \qquad (4.15)$$
$$- Te_T - EB_2\,(\theta'\phi' + \tfrac{1}{2}\phi'^2)$$

$$Q = (GJ + EB_1\,\theta'^2 + Tk_A^2)\,\phi' + Tk_A^2\,\theta'$$
$$- EB_2\,(\theta' + \phi')\,[v''\cos(\theta+\phi) + w''\sin(\theta+\phi)]$$

where:

$$EI_1 = \iint_{\text{cross-sect.}} E\zeta^2 \, d\eta \, d\zeta$$

$$EI_2 = \iint_{\text{cross-sect.}} E\eta(\eta - e_T) \, d\eta \, d\zeta$$

$$GJ = \iint_{\text{cross-sect.}} G(\eta^2 + \zeta^2) \, d\eta \, d\zeta$$

$$EB_1 = \iint_{\text{cross-sect.}} E(\eta^2 + \zeta^2)(\eta^2 + \zeta^2 - k_A^2) \, d\eta \, d\zeta$$

$$EB_2 = \iint_{\text{cross-sect.}} E(\eta^2 + \zeta^2)(\eta - e_T) \, d\eta \, d\zeta$$

4.4 Moment-Curvature Relations

Using the transformation from $\xi\eta\zeta$ to xyz and applying the ordering scheme, one arrives at the final moment-curvature relations:

$$\begin{aligned} M_x = {} & (GJ + EB_1\theta'^2 + Tk_A^2)\phi' + Tk_A^2\theta' + Te_T(w'\cos(\theta+\phi) - v'\sin(\theta+\phi)) \\ & - EB_2(\theta' + \phi')(v''\cos(\theta+\phi) + w''\sin(\theta+\phi)) \\ & + (EI_2\sin^2(\theta+\phi) + EI_1\cos^2(\theta+\phi))v'w'' \\ & - (EI_2\cos^2(\theta+\phi) + EI_1\sin^2(\theta+\phi))v''w' \\ & + (EI_2 - EI_1)\sin(\theta+\phi)\cos(\theta+\phi)[v'v'' - w'w''] \end{aligned}$$

$$M_y = (GJ + Tk_A^2)\phi'v' + Te_T^2\vartheta SIN(\theta+\phi) + EB_2(\theta'\phi' + \tfrac{1}{2}\phi'^2)SIN(\theta+\phi)$$
$$- EB_2(v'v''COS(\theta+\phi) + v'w''SIN(\theta+\phi))$$
$$- (EI_2 SIN^2(\theta+\phi) + EI_1 COS^2(\theta+\phi))w''$$
$$- (EI_2 - EI_1) SIN(\theta+\phi) COS(\theta+\phi) v''$$

$$M_z = (GJ + Tk_A^2)\phi'w' - Te_T COS(\theta+\phi) + EB_2(\theta'\phi' + \tfrac{1}{2}\phi'^2) COS(\theta+\phi)$$
$$- EB_2(w'v''COS(\theta+\phi) + w'w''SIN(\theta+\phi))$$
$$+ (EI_2 COS^2(\theta+\phi) + EI_1 SIN^2(\theta+\phi))v''$$
$$+ (EI_2 - EI_1) SIN(\theta+\phi) COS(\theta+\phi) w'' \qquad (4.16)$$

4.5 Equilibrium Equations

Figure 4.3 shows the resultant and applied forces and moments on an element of the blade. Force equilibrium gives:

$$T' + p_x = 0$$
$$V_y' + p_y = 0 \qquad (4.17)$$
$$V_z' + p_z = 0$$

Moment equilibrium gives:

$$M_x' + V_z v' - V_y w' + q_x = 0$$

$$M_y' - V_z + T w' + q_y = 0 \qquad (4.18)$$

$$M_z' + V_y - T v' + q_z = 0$$

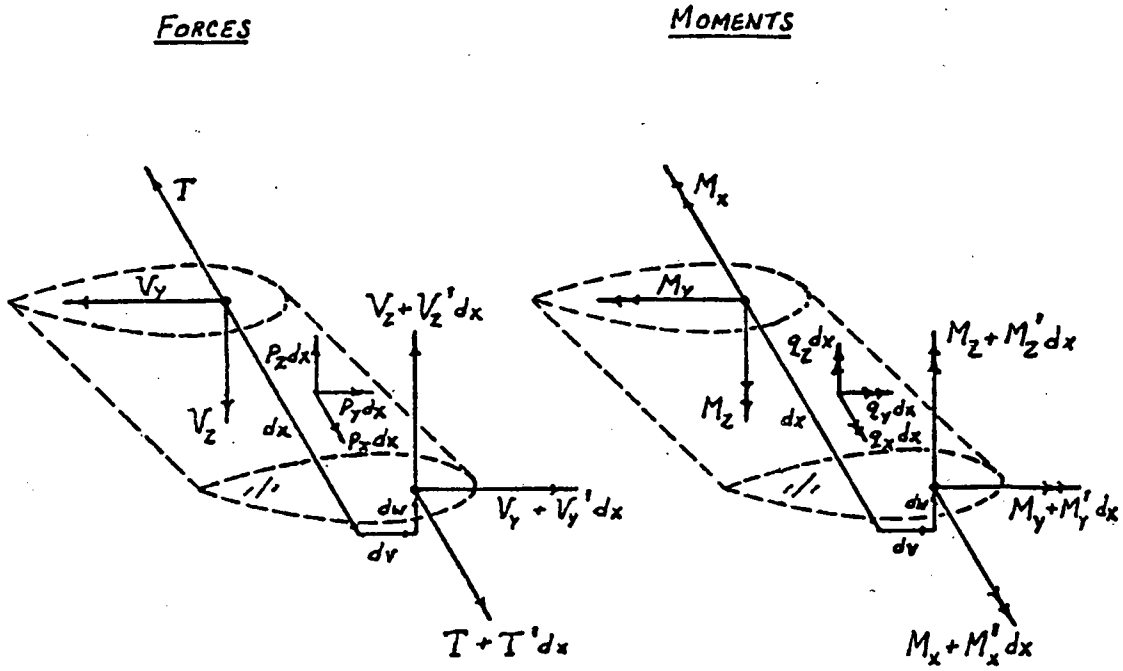

Fig. 4.3

Equations (4.17) and (4.18) may be combined to eliminate the shears V_x and V_y. Then the equilibrium equations are:

$$T' + p_x = 0$$

$$M_x' + M_y' v' + M_z' w' + q_x + q_y v' + q_z w' = 0 \qquad (4.19)$$

$$M_y'' + (T w')' + q_y' + p_z = 0$$

$$M_z'' - (T v')' + q_z' - p_y = 0$$

The applied moments, q_x, q_y, and q_z, and forces, p_x, p_y, and p_z, arise from inertia, aerodynamic and perhaps other sources. They will be derived later, in Chapters V and VI.

4.6 Final Structural Equations

Combining the moment-curvature (Eqs. (4.19)) gives the final structural equations:

$$T' + p_x = 0 \qquad (4.20)$$

$$\Big\{ (EI_2 \cos^2\theta + EI_1 \sin^2\theta) v'' + (EI_2 - EI_1)[\sin\theta\cos\theta\, w'' + -2\sin\theta\cos\theta\, \phi v'' + (\cos^2\theta - \sin^2\theta)\phi w''] - Te_T(\cos\theta - \phi\sin\theta) - EB_2\theta'\cos\theta\,\phi' \Big\}'' - \Big\{ T v' \Big\}' + q_z' - p_y = 0$$

$$\Big\{ (EI_2 \sin^2\theta + EI_1 \cos^2\theta) w'' + (EI_2 - EI_1)\,[\sin\theta\cos\theta\, v'' + -2\sin\theta\cos\theta\,\phi\, w'' + (\cos^2\theta - \sin^2\theta)\,\phi\, v''] - Te_T(\phi\cos\theta + \sin\theta) - EB_2\,\theta'\sin\theta\,\phi' \Big\}'' - \Big\{ T w' \Big\}' - q_y' - p_z = 0$$

$$- \Big\{ (GJ_E + Tk_A^2)\,\phi' + Tk_A^2\,\theta' - EB_2\,\theta'(v''\cos\theta + w''\sin\theta) \Big\}' - Te_T(w''\cos\theta - v''\sin\theta) + (EI_2 - EI_1)(\cos^2\theta - \sin^2\theta)\,v''w'' - (EI_2 - EI_1)\sin\theta\cos\theta\,(v''^2 - w''^2) - q_x - q_y v' - q_z w' = 0 \qquad (4.21)$$

where:

$$GJ_E = GJ + EB_1\,\theta'^2$$

$$EA = \iint_{\text{cross-sect.}} E\, d\eta\, d\zeta \qquad e_T = \frac{1}{EA}\iint E\,\eta\, d\eta\, d\zeta$$

$$EI_1 = \iint_{\text{cross-sect.}} E\,\zeta^2\, d\eta\, d\zeta \qquad k_A^2 = \frac{1}{EA}\iint E(\eta^2+\zeta^2)\, d\eta\, d\zeta$$

$$EI_2 = \iint E\,\eta\,(\eta - e_T)\, d\eta\, d\zeta$$

$$EB_1 = \iint E\,(\eta^2+\zeta^2)(\eta^2+\zeta^2-k_A^2)\, d\eta\, d\zeta$$

$$EB_2 = \iint E\,(\eta^2+\zeta^2)(\eta - e_T)\, d\eta\, d\zeta$$

These equations may be compared to those of Houboult and Brooks,[10] and those of Friedmann[9] or Hodges and Dowell.[7] Note the use of the standard approximations:

$$\begin{aligned} \cos(\theta+\phi) &\cong \cos\theta - \phi \sin\theta \\ \sin(\theta+\phi) &\cong \phi\cos\theta + \sin\theta \end{aligned} \tag{4.22}$$

Chapter V

Inertia Loads

The distributed inertia forces and the associated moments arising from the motion of the blade must be carefully derived to include all of the important effects. The ordering scheme becomes quite valuable here, to sort out the many terms.

5.1 Acceleration of a Point

The absolute acceleration of a point on the deformed, rotating blade is given by kinematics:

$$\vec{a} = \vec{\omega} \times (\vec{\omega} \times \vec{R}) + 2\vec{\omega} \times \dot{\vec{R}} + \ddot{\vec{R}} \tag{5.1}$$

where:

$$(\dot{}) = \frac{\partial}{\partial t}$$

From Chapter II,

$$\vec{R} = \begin{Bmatrix} X + e_x \cos\beta_p + u - \eta(v'\cos(\theta+\phi) + w'\sin(\theta+\phi)) \\ \qquad\qquad - \zeta(w'\cos(\theta+\phi) - v'\sin(\theta+\phi)) \\ e_y + v + \eta\cos(\theta+\phi) - \zeta\sin(\theta+\phi) \\ -e_x\sin\beta_p + w + \eta\sin(\theta+\phi) + \zeta\cos(\theta+\phi) \end{Bmatrix} \begin{Bmatrix} \hat{i} \\ \hat{j} \\ \hat{k} \end{Bmatrix} \tag{5.2}$$

$$\vec{\omega} = \Omega \hat{K}$$

$$= \begin{bmatrix} \Omega \sin\beta_p & 0 & \Omega \cos\beta_p \end{bmatrix} \begin{Bmatrix} \hat{i} \\ \hat{j} \\ \hat{k} \end{Bmatrix} \qquad (5.3)$$

To simplify writing, the acceleration is broken into its three components. Carrying out the vector multiplication and addition:

$$\vec{a} = a_x \hat{i} + a_y \hat{j} + a_z \hat{k} \qquad (5.4)$$

where:

$$a_x = -\Omega^2 \{ (x+u)\cos\beta_p + e_x - w\sin\beta_p - \eta [(v'\cos\theta + w'\sin\theta)\cos\beta_p + (\phi\cos\theta + \sin\theta)\sin\beta_p] - \zeta [(w'\cos\theta - v'\sin\theta)\cos\beta_p + (\cos\theta - \phi\sin\theta)\sin\beta_p] \} \cos\beta_p$$
$$-2\Omega \{ \dot{v} - \eta\dot{\phi}\sin\theta - \zeta\dot{\phi}\cos\theta \} \cos\beta_p$$
$$+ \{ \ddot{u} - \eta(\ddot{v}'\cos\theta + \ddot{w}'\sin\theta) - \zeta(\ddot{w}'\cos\theta - \ddot{v}'\sin\theta) \}$$

$$a_y = -\Omega^2 \{ e_y + v + \eta(\cos\theta - \phi\sin\theta) - \zeta(\phi\cos\theta + \sin\theta) \}$$
$$-2\Omega \{ \dot{w}\sin\beta_p + \eta[(\dot{v}'\cos\theta + \dot{w}'\sin\theta)\cos\beta_p + \dot{\phi}\cos\theta\sin\beta_p] - \dot{u}\cos\beta_p + \zeta[(\dot{w}'\cos\theta - \dot{v}'\sin\theta)\cos\beta_p - \dot{\phi}\sin\theta\sin\beta_p] \}$$
$$+ \{ \ddot{v} - \eta\ddot{\phi}\sin\theta - \zeta\ddot{\phi}\cos\theta \}$$

$$
\begin{aligned}
a_z = \; & -\Omega^2 \Big\{ -(X+u)\cos\beta_p - e_x + w\sin\beta_p \\
& \quad + \eta\left[(v'\cos\theta + w'\sin\theta)\cos\beta_p + (\phi\cos\theta + \sin\theta)\sin\beta_p\right] \\
& \quad + \zeta\left[(w'\cos\theta - v'\sin\theta)\cos\beta_p + (\cos\theta - \phi\sin\theta)\sin\beta_p\right]\Big\}\sin\beta_p \\
& -2\Omega\left\{-\dot{v} + \eta\dot{\phi}\sin\theta + \zeta\dot{\phi}\cos\theta\right\}\sin\beta_p \\
& + \left\{\ddot{w} + \eta\ddot{\phi}\cos\theta - \zeta\ddot{\phi}\sin\theta\right\}
\end{aligned}
$$

5.2 Distributed Forces

Each particle of the blade cross-section undergoes the acceleration given by Eq. (5.4). D'Alembert's Principle may be used to find the infinitesimal force of inertia on a particle as:

$$d\bar{p}^I = -\hat{a}\, dm = -\hat{a}\, \rho_b\, d\eta\, d\zeta \tag{5.5}$$

where:

$$\rho_b = \text{BLADE MATERIAL DENSITY}$$

Integrating over the cross-section, and again dividing into three components gives the distributed forces due to inertia:

$$p_x^I = m\Omega^2 \left[(1-\beta_p^2)x + e_x + 2\dot{v}/\Omega \right]$$

$$p_y^I = m\Omega^2 \left[e_Y + e_I \cos\theta + v - e_I \sin\theta\, \phi \right. \tag{5.6}$$
$$+ (-2\dot{u} + 2\beta_p \dot{w} + 2e_I \cos\theta\, \dot{v}' + 2e_I \sin\theta\, \dot{w}')/\Omega$$
$$\left. + (-\ddot{v} + e_I \sin\theta\, \ddot{\phi})/\Omega^2 \right]$$

$$p_z^I = m\Omega^2 \left[-\beta_p (x+e_x) - 2\beta_p \dot{v}/\Omega - (\ddot{w} + e_I \cos\theta\, \ddot{\phi})/\Omega^2 \right]$$

where:

$$m = \iint_{\text{cross-sect.}} \rho_b\, d\eta\, d\zeta$$

$$e_I = \frac{1}{m} \iint_{\text{cross-sect.}} \rho_b\, \eta\, d\eta\, d\zeta$$

SYMMETRY:

$$\iint_{\text{cross-sect.}} \rho_b\, \zeta\, d\eta\, d\zeta = 0$$

5.3 Distributed Moments

Given the radius to a point on the blade cross-section and the infinitesimal force there, the moment due to that force is:

$$d\vec{q}^I = \vec{r}_c \times d\vec{p}^I = (\vec{r}_c \times \vec{a})\rho_b \, d\eta \, d\zeta \tag{5.7}$$

Recall from Chapter II that the radius within the cross-section is given as:

$$\vec{r}_c = \begin{Bmatrix} -\eta(v'\cos(\theta+\phi)+w'\sin(\theta+\phi)) - \zeta(w'\cos(\theta+\phi)-v'\sin(\theta+\phi)) \\ \eta\cos(\theta+\phi) - \zeta\sin(\theta+\phi) \\ \eta\sin(\theta+\phi) + \zeta\cos(\theta+\phi) \end{Bmatrix}^T \begin{Bmatrix} \hat{i} \\ \hat{j} \\ \hat{k} \end{Bmatrix} \tag{5.8}$$

Performing the vector multiplication, integrating over the cross-section, and separating components gives the distributed moments due to rotation:

$$\begin{aligned} q_x^I = m\Omega^2 [& -\beta_p e_I x \cos\theta - e_I e_y \sin\theta - (k_{m2}^2 - k_{m1}^2)\sin\theta\cos\theta \\ & - e_I \sin\theta \, v - (k_{m2}^2 - k_{m1}^2)(\cos^2\theta - \sin^2\theta)\phi \\ & + (e_I \sin\theta \, \ddot{v} - e_I \cos\theta \, \ddot{w} - (k_{m2}^2 + k_{m1}^2)\ddot{\phi})/\Omega^2] \end{aligned} \tag{5.9}$$

$$q_y^I = m\Omega^2 [e_I x \sin\theta + e_I e_x \sin\theta + e_I x \cos\theta \, \phi + 2 e_I \sin\theta \, \dot{v}/\Omega]$$

$$q_z^I = m\Omega^2 [-e_I x \cos\theta - e_I e_x \cos\theta + e_I x \sin\theta \, \phi - 2 e_I \cos\theta \, \dot{v}/\Omega]$$

where: $$k_{m_1}^2 = \frac{1}{m}\iint_{\text{cross-sect.}} \rho_b \zeta^2 d\eta d\zeta$$

$$k_{m_2}^2 = \frac{1}{m}\iint_{\text{cross-sect.}} \rho_b \eta^2 d\eta d\zeta$$

$$\left(k_{m_2}^2 + k_{m_1}^2 = k_m^2 \right)$$

As in Chapter IV, $\cos(\theta + \phi)$ and $\sin(\theta + \phi)$ have been expanded here.

Chapter VI

Aerodynamic Loads

Aerodynamic forces and moments on the blades arise due to the airflow relative to the blade. The airflow results from blade rotation and flexure, and from the inflow of air through the wind turbine. As Friedmann[11] has pointed out, the rotor blade has three important degrees of freedom, u, w, and ϕ, so that Theodorsen's[12] unsteady aerodynamics are not strictly applicable. Rather, the modified results of Greenberg[13] are used.

For the purpose of this work, quasisteady aerodynamics ($C(k) = 1$) were deemed adequate. Indeed, Miller and Ellis[14] have shown that results are conservative when this simplification is employed.

6.1 Blade Relative Velocity

It is convenient to introduce a fourth coordinate system, cartesian x_2 y_2 z_2 (Fig. 6.1), which is parallel to xyz, but moves with the deformed blade. Unit vectors are $\hat{i}_2$, $\hat{j}_2$, $\hat{k}_2$ and the incidence angle between y_2 and η is θ_i. To second order:

$$\theta_i = \theta + \phi \tag{6.1}$$

The corresponding transformation is:

$$\begin{Bmatrix} \hat{i}_2 \\ \hat{j}_2 \\ \hat{k}_2 \end{Bmatrix} = \begin{bmatrix} 1 & v' & w' \\ -v' & 1 & 0 \\ -w' & 0 & 1 \end{bmatrix} \begin{Bmatrix} \hat{i} \\ \hat{j} \\ \hat{k} \end{Bmatrix} \tag{6.2}$$

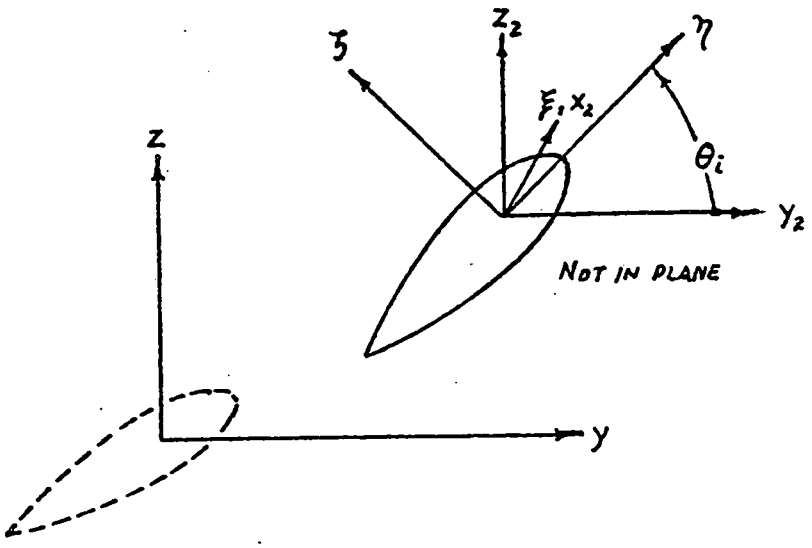

Fig. 6.1

The blade velocity relative to the air is given by kinematics:

$$\vec{U} = \vec{\omega} \times \vec{R} + \dot{\vec{R}} - \vec{u}_{inflow} \tag{6.3}$$

The velocity of the air is:

$$\vec{u}_{inflow} = \lambda \Omega R_T \hat{K}$$

$$= \begin{bmatrix} \lambda\Omega R_T \sin\beta_p & 0 & \lambda\Omega R_T \cos\beta_p \end{bmatrix} \begin{Bmatrix} \hat{i} \\ \hat{j} \\ \hat{k} \end{Bmatrix} \quad (6.4)$$

where:

$$\lambda = \frac{u_{inflow}}{\Omega R_T}$$

R_T = TIP RADIUS

Recall Eqs. (2.4) and (5.3):

$$\vec{R} = \begin{Bmatrix} x + e_x \cos\beta_p + u - \eta(v'\cos(\theta+\phi) + w'\sin(\theta+\phi)) \\ \qquad - \zeta(w'\cos(\theta+\phi) - v'\sin(\theta+\phi)) \\ e_Y + v + \eta\cos(\theta+\phi) - \zeta\sin(\theta+\phi) \\ -e_x \sin\beta_p + w + \eta\sin(\theta+\phi) + \zeta\cos(\theta+\phi) \end{Bmatrix}^T \begin{Bmatrix} \hat{i} \\ \hat{j} \\ \hat{k} \end{Bmatrix} \quad (6.5)$$

$$\vec{\omega} = \Omega \sin\beta_p \hat{i} + \Omega \cos\beta_p \hat{k} \quad (6.6)$$

Then, carrying out the vector multiplication and addition, and transforming to the x_2 y_2 z_2 coordinate system gives:

$$\vec{U} = U_{y_2} \hat{j}_2 + U_{z_2} \hat{k}_2 \quad (6.7)$$

where

$$U_{y_2} = \dot{v} + \Omega x \cos\beta_p + \Omega e_x$$

$$U_{z_2} = \dot{w} + \lambda\Omega R_T \cos\beta_p + \Omega(\beta_p + w')(v + e_Y)$$

Note that the cross flow parallel to the deformed blade is ignored. The magnitude of the velocity $\vec{U}$ is calculated using the approximation $\sqrt{1+\varepsilon_0} \cong 1 + 1/2\ \varepsilon_0$:

$$|\vec{U}| = U = \Omega x \cos\beta_p + \Omega e_x + \frac{1}{2}\lambda^2\Omega\frac{R_T^2}{x}\cos\beta_p + \dot{v} + \lambda\frac{R_T}{x}\dot{w} \quad (6.8)$$

The blade relative velocity is now manipulated into a form compatible with Greenberg's[13] theory. First, the velocity is separated into a steady part, $\vec{V}_0$, and a time varying part, $\vec{v}$ (Fig. 6.2):

$$\vec{U} = \vec{V}_o + \vec{v}(t) \quad (6.9)$$

where:

$$\vec{V}_o = [\Omega x \cos\beta_p + \Omega e_x]\hat{j}_2 + [\lambda\Omega R_T \cos\beta_p + \Omega\beta_p e_Y]\hat{k}_2$$

$$\vec{v} \cong \dot{v}\,\hat{j}_2 + \dot{w}\,\hat{k}_2$$

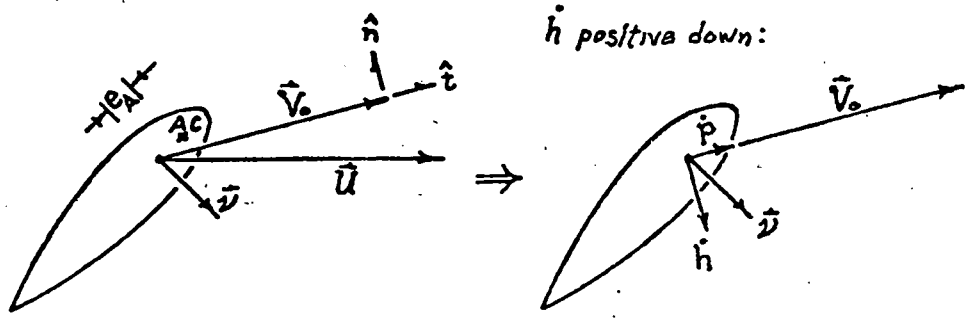

Fig. 6.2

Further, the time varying part of the velocity is separated into a component perpendicular to V_0, $\dot{h}$, and a component parallel to V_0, $\dot{p}$. This is accomplished by defining a unit vector tangent to V_0, $\hat{t}$, and a unit vector normal to V_0, $\hat{n}$. Using the expansion $1/\sqrt{1+\varepsilon_0} = 1 - 1/2\ \varepsilon_0$:

$$\frac{1}{|\vec{V}_0|} \equiv \frac{1}{\Omega x \cos\beta_p}\left\{1 - \frac{e_x}{x\cos\beta_p} - \frac{1}{2}\lambda^2\frac{R_T^2}{x^2}\right\} \tag{6.10}$$

Then:

$$\hat{t} = \frac{\vec{V}_0}{|\vec{V}_0|} = \left[1 - \tfrac{1}{2}\lambda^2\frac{R_T^2}{x^2}\right]\hat{j}_2 + \left[\lambda\frac{R_T}{x} - \frac{\lambda e_x R_T}{x^2\cos\beta_p}\right]\hat{k}_2 \tag{6.11}$$

And, by inspection:

$$\hat{n} = -\left[\lambda\frac{R_T}{x} - \frac{\lambda e_x R_T}{x^2\cos\beta_p}\right]\hat{j}_2 + \left[1 - \tfrac{1}{2}\lambda^2\frac{R_T^2}{x^2}\right]\hat{k}_2 \tag{6.12}$$

Now, $\dot{h}$ and $\dot{p}$ are simply:

$$\dot{h} = -\hat{n}\cdot\vec{v} = -\left(1 - \tfrac{1}{2}\lambda^2\frac{R_T^2}{x^2}\right)\dot{w} + \lambda\frac{R_T}{x}\dot{v} \tag{6.13}$$

$$\dot{p} = \hat{t}\cdot\vec{v} = \left(1 - \tfrac{1}{2}\lambda^2\frac{R_T^2}{x^2}\right)\dot{v} + \lambda\frac{R_T}{x}\dot{w} \tag{6.14}$$

Finally, the steady velocity and the pulsation ($\dot{p}$) are added to give the total velocity:

$$\begin{aligned}\vec{V} &= \vec{V}_o + \dot{p}\,\hat{t} \\ &= V_{y2}\,\hat{j}_2 + V_{z2}\,\hat{k}_2\end{aligned} \tag{6.15}$$

where:

$$V_{y_2} = \Omega x \cos\beta_p + \Omega e_x + \dot{v} + \lambda \frac{R_T}{x} \dot{w}$$

$$V_{z_2} = \lambda \Omega R_T \cos\beta_p + \Omega (\beta_p + w')(v + e_y) + \lambda \frac{R_T}{x} \dot{v}$$

The magnitude of $\vec{V}$ and its inverse are:

$$|\vec{V}| = V \cong \Omega x \cos\beta_p + \Omega e_x + \frac{1}{2} \lambda^2 \frac{R_T^2}{x} \cos\beta_p + \dot{v} \qquad (6.16)$$

$$\frac{1}{V} \cong \frac{1}{\Omega x \cos\beta_p} \left\{ 1 - \frac{e_x}{x \cos\beta_p} - \frac{1}{2} \lambda^2 \frac{R_T^2}{x^2} - \frac{\dot{v}}{\Omega x \cos\beta_p} \right\}$$

The time derivative of $\vec{V}$ is simply:

$$\dot{V} = \frac{\partial \dot{p}}{\partial t} = \left(1 - \frac{1}{2} \lambda^2 \frac{R_T^2}{x^2}\right) \ddot{v} + \lambda \frac{R_T}{x} \ddot{w} \qquad (6.17)$$

Also:

$$\ddot{h} = \frac{\partial \dot{h}}{\partial t} = -\left(1 - \frac{1}{2} \lambda^2 \frac{R_T^2}{x^2}\right) \ddot{w} + \lambda \frac{R_T}{x} \ddot{v} \qquad (6.18)$$

6.2 Angle of Attack

The velocity vector $\vec{V}$ and the blade chord define the angle of attack α as shown in Fig. 6.3. This angle is regarded as small, and may be related to the components V_{y_2} and V_{z_2} as follows:

$$\frac{V_{z_2}}{V} = \sin(\theta_i - \alpha) = \sin\theta_i \cos\alpha - \cos\theta_i \sin\alpha$$

$$\frac{V_{y_2}}{V} = \cos(\theta_i - \alpha) = \cos\theta_i \cos\alpha + \sin\theta_i \sin\alpha \qquad (6.19)$$

Now solve for α after applying the small angle approximations:

$$\cos\alpha \cong 1 \qquad \sin\alpha \cong \alpha \qquad (6.20)$$

Then:

$$\alpha = \frac{V_{y_2}}{V} \sin\theta_i - \frac{V_{z_2}}{V} \cos\theta_i \qquad (6.21)$$

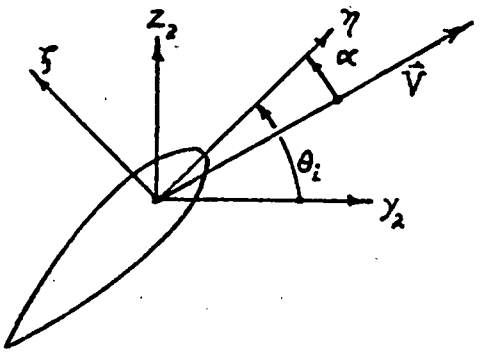

Fig. 6.3

The angular velocity of the blade section about the x_2 axis must include the component of ω along the x_2 axis. To second order:

$$\dot{\alpha} = \dot{\phi} + \Omega(\beta_p + w') \qquad (6.22)$$

Differentiating with respect to time:

$$\ddot{\alpha} = \ddot{\phi} + \Omega \dot{w}' \tag{6.23}$$

6.3 Quasisteady Aerodynamic Loads

Greenberg's[13] results for C(k) = 1, and translated into the present notation, are:

$$\ell_{nc} = \frac{\rho a c}{2} \frac{c}{4} \left\{ \ddot{h} + V\dot{\alpha} + \dot{V}\alpha + \left(\frac{c}{4} - e_A\right)\ddot{\alpha} \right\} \tag{6.24}$$

$$\ell_c = \frac{\rho a c}{2} V \left\{ V\alpha + \left(\frac{c}{2} - e_A\right)\dot{\alpha} + \dot{h} \right\} \tag{6.25}$$

$$m_{EA} = -\frac{\rho a c}{2} \frac{c}{4} \left\{ \left(\frac{c}{2} - e_A\right) V\dot{\alpha} + \left(\frac{c}{4} - e_A\right)\left(\dot{V}\alpha + \ddot{h}\right) + \left(\frac{3}{8}\frac{c^2}{4} - \frac{c}{2}e_A + e_A^2\right)\ddot{\alpha} \right\} + \frac{\rho a c}{2} e_A V \left\{ V\alpha + \left(\frac{c}{2} - e_A\right)\dot{\alpha} + \dot{h} \right\} \tag{6.26}$$

Also:

$$d = \frac{\rho a c}{2} \frac{c_{d_0}}{a} U^2 \tag{6.27}$$

The lift has been divided into non-circulatory and circulatory parts. These are distributed forces and moments which act on the blade as shown in Fig. 6.4. Note that the circulatory lift is defined perpendicular to the U vector, while the noncirculatory lift is defined normal to the chord.[8] The drag is tangent to the U vector, and the pitching moment acts about the x_2 axis.

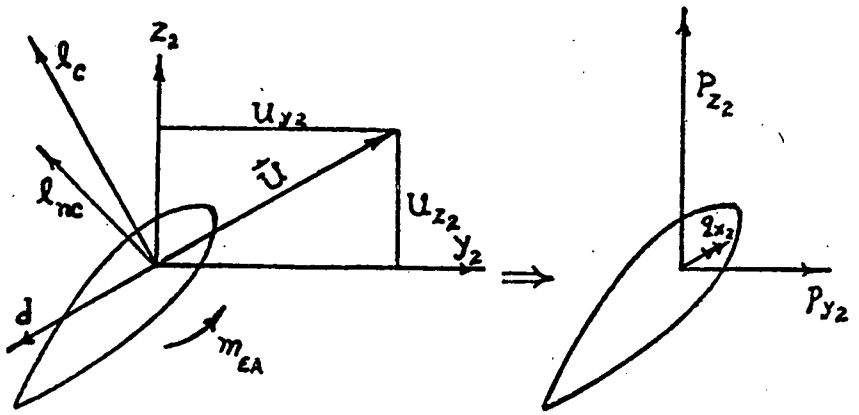

Fig. 6.4

The components of the net distributed force in the y_2 and z_2 directions are found by inspection:

$$p_{y_2} = -d\frac{u_{y_2}}{u} - \ell_c\frac{u_{z_2}}{u} - \ell_{nc}\sin\theta_i$$

$$p_{z_2} = -d\frac{u_{z_2}}{u} + \ell_c\frac{u_{y_2}}{u} + \ell_{nc}\cos\theta_i \qquad (6.28)$$

Also:

$$q_{xz} = m_{EA} \qquad (6.29)$$

Substituting ℓ_{nc}, ℓ_c, and d into Eqs. (6.28) and substituting for α (Eq. (6.21)), then transforming into the xyz coordinate system gives:

$$p_x^A \equiv 0$$

$$p_y^A = -\frac{\rho a c}{2}\left\{\frac{c_{D_0}}{a} U U_{y_2} + U_{z_2} V_{y_2} \sin(\theta+\phi) - U_{z_2} V_{z_2} \cos(\theta+\phi) \right.$$
$$+ \left(\frac{c}{2} - e_A\right) U_{z_2} \dot{\alpha} + U_{z_2} \dot{h} + \frac{c}{4} \ddot{h} \sin(\theta+\phi)$$
$$+ \frac{c}{4} V \dot{\alpha} \sin(\theta+\phi) + \frac{c}{4} \ddot{p} \frac{V_{y_2}}{V} \sin^2(\theta+\phi)$$
$$\left. - \frac{c}{4} \ddot{p} \frac{V_{z_2}}{V} \sin(\theta+\phi)\cos(\theta+\phi) + \frac{c}{4}\left(\frac{c}{4} - e_A\right) \ddot{\alpha} \sin(\theta+\phi) \right\}$$

$$p_z^A = \frac{\rho a c}{2}\left\{ U_{y_2} V_{y_2} \sin(\theta+\phi) - U_{y_2} V_{z_2} \cos(\theta+\phi) + U_{y_2} \dot{h} \right. \qquad (6.30)$$
$$+ \left(\frac{c}{2} - e_A\right) U_{y_2} \dot{\alpha} - \frac{c_{D_0}}{a} U U_{z_2} + \frac{c}{4} \ddot{h} \cos(\theta+\phi)$$
$$+ \frac{c}{4} V \dot{\alpha} \cos(\theta+\phi) + \frac{c}{4} \ddot{p} \frac{V_{y_2}}{V} \sin(\theta+\phi)\cos(\theta+\phi)$$
$$\left. - \frac{c}{4} \ddot{p} \frac{V_{z_2}}{V} \cos^2(\theta+\phi) + \frac{c}{4}\left(\frac{c}{4} - e_A\right) \ddot{\alpha} \cos(\theta+\phi) \right\}$$

Similarly for Eq. (6.29):

$$q_x^A = \frac{\rho a c}{2}\left\{ -\frac{c}{4}\left(\frac{c}{2} - e_A\right) V \dot{\alpha} - \frac{c}{4}\left(\frac{3}{8}\frac{c^2}{4} - \frac{c}{2} e_A + e_A^2\right) \ddot{\alpha} \right.$$
$$- \frac{c}{4}\left(\frac{c}{4} - e_A\right)\left[\ddot{p} \frac{V_{y_2}}{V} \sin(\theta+\phi) - \ddot{p} \frac{V_{z_2}}{V} \cos(\theta+\phi) + \ddot{h}\right]$$
$$+ e_A V V_{y_2} \sin(\theta+\phi) - e_A V V_{z_2} \cos(\theta+\phi) \qquad (6.31)$$
$$\left. + e_A\left(\frac{c}{2} - e_A\right) V \dot{\alpha} + e_A V \dot{h} \right\}$$

$$q_y^A \cong q_x^A v'$$

$$q_z^A \cong q_x^A w'$$

Finally, substituting for the various velocity components yields the distributed aerodynamic forces:

$$P_x^{\wedge} \cong 0$$

$$\begin{aligned} P_y^{\wedge} = \frac{\rho a c}{2}\Omega^2 \Big\{ & \lambda^2 R_T^2 \cos\theta - \lambda(1-\beta_p^2) R_T x \sin\theta \\ & - \lambda R_T e_x \sin\theta - \frac{C_{D_0}}{a} x^2 - \lambda R_T x \cos\theta\, \phi \\ & - \left[\lambda R_T \sin\theta + 2\frac{C_{D_0}}{a} x\right] \dot{v}/\Omega \\ & - \left[x\sin\theta - \lambda R_T(1+\cos\theta)\right] \dot{w}/\Omega \\ & - \left(\tfrac{c}{4}\sin^2\theta\, \ddot{v} + \tfrac{c}{4}\sin\theta\, \ddot{w}\right)/\Omega^2 \Big\} \end{aligned} \qquad (6.32)$$

$$\begin{aligned} P_z^{\wedge} = \frac{\rho a c}{2}\Omega^2 \Big\{ & (1-\beta_p^2) x^2 \sin\theta + 2 e_x x \sin\theta - \lambda R_T (x+e_x)\cos\theta \\ & - \beta_p e_y x + \left(\tfrac{c}{2} + \tfrac{c}{4}\cos\theta - e_A\right)\beta_p x - x(\beta_p + w')v \\ & - e_y x w' + x^2 \cos\theta\, \phi + \left(\tfrac{c}{2} + \tfrac{c}{4}\cos\theta - e_A\right) x w' \\ & + \left(\tfrac{c}{2} + \tfrac{c}{4}\cos\theta - e_A\right) x \dot{\phi}/\Omega - \left[x - \lambda R_T \sin\theta\right]\dot{w}/\Omega \\ & + \left[2x\sin\theta - \lambda R_T(2\cos\theta - 1)\right]\dot{v}/\Omega \\ & + \left(\tfrac{c}{4}\sin\theta\cos\theta\, \ddot{v} - \tfrac{c}{4}\cos\theta\, \ddot{w}\right)/\Omega^2 \Big\} \end{aligned}$$

And the distributed aerodynamic moments:

$$q_x^A = \frac{\rho a c}{2}\Omega^2\Big\{e_A(1-\beta_p^2)x^2\sin\theta + 2e_A e_x x\sin\theta - e_A\lambda R_T x\cos\theta + \tfrac{1}{2}e_A\lambda^2 R_T^2\cos\theta + (2e_A x\sin\theta\,\dot{v} - e_A x\dot{w})/\Omega - (\tfrac{c}{4}-e_A)(\tfrac{c}{2}-e_A)x\dot{\phi}/\Omega\Big\} \tag{6.33}$$

$$q_y^A = \frac{\rho a c}{2}\Omega^2 e_A x^2\sin\theta\, v'$$

$$q_z^A = \frac{\rho a c}{2}\Omega^2 e_A x^2\sin\theta\, w'$$

The usual expansions for $\sin(\theta + \phi)$ and $\cos(\theta + \phi)$ are used. The ordering scheme has been relaxed to include some seemingly small damping terms which may be important in certain cases.[8]

Chapter VII

Final Governing Differential Equations

All that remains is to place the distributed loads and moments into the final structural equations. However, it is convenient to first establish the dependence of T and u on v, w, and ϕ. To do this, one follows the procedure of Hodges and Ormiston,[8] taking:

$$\frac{m\Omega^2 L^2}{EA} = O(\epsilon_o^2) \tag{7.1}$$

This assumption is reasonable for most wind turbines: blade stretching due to the tension is negligible.

Placing p_x (Eqs. (5.6) and (6.32)) into Eq. (4.20):

$$T' + m\Omega^2 \left\{ \cos^2\beta_p \, x + e_x + 2\dot{v}/\Omega \right\} \tag{7.2}$$

Integrating from x to L:

$$T = \Omega^2 \left\{ (1-\beta_p^2) \int_x^L m x \, dx + e_x \int_x^L m \, dx + \frac{2}{\Omega} \int_x^L m \dot{v} \, dx \right\} \tag{7.3}$$

where T(L) is taken to be zero. This equation is used to find T when solving the equations. Now, recall Eq. (4.9):

$$T = EA \left\{ u' + \frac{1}{2} v'^2 + \frac{1}{2} w'^2 + k_A^2 \theta' \phi' - e_T (v'' \cos\theta + w'' \sin\theta) \right\} \tag{7.4}$$

Equating with Eq. (7.3), and solving for u':

$$u'' = \frac{\Omega^2}{EA}\int_x^L m x\,dx - \frac{1}{2}v'^2 - \frac{1}{2}w'^2 + e_T(v''\cos\theta + w''\sin\theta) \tag{7.5}$$

All terms of $0(\varepsilon_0^3)$ or higher have been discarded, since u appears in Eq. (5.6), where terms up to $0(\varepsilon_0^2)$ only are retained. Finally, integrating from 0 to x, then differentiating with respect to time yields:

$$\ddot{u} = -\int_0^x (v'\ddot{v}' + w'\ddot{w}')\,dx + \int_0^x e_T(\ddot{v}''\cos\theta + \ddot{w}''\sin\theta)\,dx \tag{7.6}$$

where u(0) is taken to be zero.

7.1 Final Dimensional Governing Equations

Combining Eqs. (4.21) with Eqs. (5.6,5.9,6.32,6.33):

$$\begin{aligned}
V:\ &\Big\{(EI_2\cos^2\theta + EI_1\sin^2\theta)v'' + (EI_2 - EI_1)[\sin\theta\cos\theta\, w'' + \\
&-2\sin\theta\cos\theta\,\phi v'' + (\cos^2\theta - \sin^2\theta)\phi w''] - Te_T(\cos\theta - \phi\sin\theta) \\
&-EB_2\theta'\cos\theta\,\phi'\Big\}'' - \{Tv'\}' + \Big\{\frac{\rho ac}{2}\Omega^2 e_A x^2\sin\theta w' \qquad (7.7)\\
&+ m\Omega^2[e_I x\sin\theta\,\phi - 2e_I\cos\theta\,\dot{v}/\Omega]\Big\}' - m\Omega^2\Big\{v - e_I\sin\theta\,\phi \\
&+ (-2\dot{u} + 2\beta_p\dot{w} + 2e_I\cos\theta\,\dot{v}' + 2e_I\sin\theta\,\dot{w}')/\Omega + (e_I\sin\theta\,\ddot{\phi} - \ddot{v})/\Omega^2\Big\} \\
&+ \frac{\rho ac}{2}\Omega^2\Big\{\lambda R_T x\cos\theta\,\phi + [\lambda R_T\sin\theta + 2\frac{c_{do}}{a}x]\dot{v}/\Omega \\
&+ [x\sin\theta - \lambda R_T(1+\cos\theta)]\dot{w}/\Omega + (\frac{c}{4}\sin^2\theta\,\ddot{v} - \frac{c}{4}\sin\theta\,\ddot{w})/\Omega^2\Big\} \\
&= \Big\{m\Omega^2[e_I x\cos\theta + e_I e_x\cos\theta]\Big\}' + m\Omega^2\{e_Y + e_I\cos\theta\} \\
&+ \frac{\rho ac}{2}\Omega^2\Big\{\lambda^2 R_T^2\cos\theta - \lambda(1-\beta_p^2)R_T x\sin\theta - \lambda R_T e_x\sin\theta - \frac{c_{do}}{a}x^2\Big\}
\end{aligned}$$

$$w:\ \Big\{ (EI_2 \sin^2\theta + EI_1 \cos^2\theta)\, w'' + (EI_2 - EI_1)[\sin\theta\cos\theta\, v'' + 2\sin\theta\cos\theta\, \phi w'' + (\cos^2\theta - \sin^2\theta)\phi v''] - Te_T(\phi\cos\theta + \sin\theta) - EB_2\,\theta'\sin\theta\,\phi' \Big\}'' - \Big\{ T w' \Big\}'$$
$$- \Big\{ m\Omega^2 [e_I x \cos\theta\,\phi + 2 e_I \sin\theta\, \dot{v}/\Omega] + \frac{\rho a c}{2}\Omega^2 e_A x^2 \sin\theta\, v' \Big\}'$$
$$+ m\Omega^2 \Big\{ 2\beta_p \dot{v}/\Omega + (\ddot{w} + e_I \cos\theta\, \ddot{\phi})/\Omega^2 \Big\}$$
$$+ \frac{\rho a c}{2}\Omega^2 \Big\{ x(\beta_p + w')v + e_T x w' - x^2 \cos\theta\,\phi - (\tfrac{c}{2} + \tfrac{c}{4}\cos\theta - e_A) x w'$$
$$- (\tfrac{c}{2} + \tfrac{c}{4}\cos\theta - e_A) x\dot{\phi}/\Omega - [2x\sin\theta - \lambda R_T(2\cos\theta - 1)]\dot{v}/\Omega$$
$$+ [x - \lambda R_T \sin\theta]\dot{w}/\Omega - (\tfrac{c}{4}\sin\theta\cos\theta\,\ddot{v} + \tfrac{c}{4}\cos\theta\,\ddot{w})/\Omega^2 \Big\}$$
$$= \Big\{ m\Omega^2 [e_I x \sin\theta + e_I e_x \sin\theta] \Big\}' - m\Omega^2 \beta_p (x + e_x)$$
$$+ \frac{\rho a c}{2}\Omega^2 \Big\{ (1 - \beta_p^2) x^2 \sin\theta + 2 e_x x \sin\theta - \lambda R_T (x + e_x)\cos\theta$$
$$- \beta_p e_T x + (\tfrac{c}{2} + \tfrac{c}{4}\cos\theta - e_A)\beta_p x \Big\}$$

$$\phi:\ -\Big\{ (GJ_E + T k_A^2)\phi' - EB_2\,\theta'(v''\cos\theta + w''\sin\theta) \Big\}' - Te_T(w''\cos\theta - v''\sin\theta)$$
$$+ (EI_2 - EI_1)[(\cos^2\theta - \sin^2\theta)v''w'' - \sin\theta\cos\theta\,(v''^2 - w''^2)]$$
$$+ m\Omega^2 \Big\{ e_I \sin\theta\, v + (k_{m2}^2 - k_{m1}^2)(\cos^2\theta - \sin^2\theta)\phi$$
$$+ (-e_I \sin\theta\,\ddot{v} + e_I \cos\theta\,\ddot{w} + (k_{m2}^2 + k_{m1}^2)\ddot{\phi})/\Omega^2 \Big\}$$
$$+ \frac{\rho a c}{2}\Omega^2 \Big\{ -2 e_A x \sin\theta\, \dot{v}/\Omega + e_A x \dot{w}/\Omega + (\tfrac{c}{4} - e_A)(\tfrac{c}{2} - e_A) x\dot{\phi}/\Omega \Big\}$$
$$+ m\Omega^2 \Big\{ -e_I x \sin\theta\, v' + e_I x \cos\theta\, w' \Big\}$$
$$= \Big\{ T k_A^2 \theta' \Big\}' - m\Omega^2 \Big\{ \beta_p e_I x \cos\theta + e_I e_T \sin\theta$$
$$+ (k_{m2}^2 - k_{m1}^2)\sin\theta\cos\theta \Big\} + \frac{\rho a c}{2}\Omega^2 \Big\{ e_A (1 - \beta_p^2) x^2 \sin\theta$$
$$+ 2 e_A e_x x \sin\theta - e_A \lambda R_T x \cos\theta + \tfrac{1}{2} e_A \lambda^2 R_T^2 \cos\theta \Big\}$$

where, to summarize:

$$GJ_e = GJ + EB_1\theta'^2$$

$$EA = \iint_{\text{cross-section}} E\,d\eta\,d\zeta$$

$$EI_1 = \iint E\zeta^2 d\eta d\zeta$$

$$EI_2 = \iint E\eta(\eta - e_T)\,d\eta d\zeta$$

$$EB_1 = \iint E(\eta^2+\zeta^2)(\eta^2+\zeta^2-k_A^2)\,d\eta d\zeta$$

$$EB_2 = \iint E(\eta^2+\zeta^2)(\eta - e_T)\,d\eta d\zeta$$

$$e_T = \frac{1}{EA}\iint E\eta\,d\eta d\zeta$$

$$k_A^2 = \frac{1}{EA}\iint E(\eta^2+\zeta^2)\,d\eta d\zeta$$

$$m = \iint \rho_b\,d\eta d\zeta$$

$$e_I = \frac{1}{m}\iint \rho_b \eta\,d\eta d\zeta$$

$$k_{m1}^2 = \frac{1}{m}\iint \rho_b \zeta^2 d\eta d\zeta$$

$$k_{m2}^2 = \frac{1}{m}\iint \rho_b \eta^2 d\eta d\zeta$$

$$\lambda = \frac{u_{inflow}}{\Omega R_T}$$

These equations may be compared to those of Hodges and Ormiston,[8] or Friedmann.[15] Note that in the former work, θ is regarded as small, whereas the present equations retain $\cos\theta$ and $\sin\theta$.

Typical boundary conditions, which apply to the large NASA wind turbines are:[4]

$$V(0) = V'(0) = w(0) = w'(0) = 0$$

$$V''(L) = V'''(L) = w''(L) = w'''(0) = \phi'(L) = 0$$

$$K_R \phi(0) = Q(0) \cong \left[(GJ_E + Tk_A^2)\phi' + Tk_A^2\theta' \right]\Big|_{x=0} \qquad (7.8)$$

where K_R is the root spring, or control system, stiffness.

PART B

AEROELASTIC STABILITY STUDY

Chapter VIII

Generalized Coordinates

Part B will pursue the solution of the equations of motion for a specific machine: the NASA-ERDA 100 kw wind turbine. However, the results of this chapter may, in general, be applied to other wind turbines with cantilever roots. The familiar Galerkin assumed mode approach is used,[18] with one mode each for u, w, and ϕ.

8.1 Assumed Modes

Assume that the variables v, w, and ϕ can be represented by the product of a shape function of x and a time varying amplitude:

$$\begin{aligned} V &= L\, \gamma_v(x)\, q_v(t) \\ W &= L\, \gamma_w(x)\, q_w(t) \\ \phi &= \gamma_\phi(x)\, q_\phi(t) \end{aligned} \tag{8.1}$$

The factor L is employed to make all of the q's non-dimensional. These generalized coordinates will now describe the deflection and behavior of the blade. Substituting this representation into the boundary conditions (Eqs. (7.8)) gives:

$$\gamma_v(0) = \gamma_v''(0) = \gamma_w(0) = \gamma_w'(0) = 0$$

$$\gamma_v''(L) = \gamma_v'''(L) = \gamma_w''(L) = \gamma_w'''(L) = \gamma_\phi'(L) = 0 \qquad (8.2)$$

$$K_R \gamma_\phi(0) \cong (GJ_E + T k_A^2) \Big|_{x=0} \gamma_\phi'(0)$$

8.2 Modal Equations

Because the algebra of this process is extensive yet straightforward, the step by step details are not included. The modal equations are simply written out, with several notes on their formation. After substituting Eqs. (8.1) into the equations of motion (Eqs. (7.7)), each equation is multiplied through by the proper weighting function and integrated over the blade from 0 to L; the v equation is weighted by $L\gamma_v$, the w equation by $L\gamma_w$, and the ϕ equation by γ_ϕ. The generalized coordinates and their time derivatives may be taken outside of the integrals; the result is a set of three coupled algebraic equations.

At this point it is prudent to non-dimensionalize the equations, by dividing through by

$$\Omega^2 I_\beta = \Omega^2 \int_0^L m x^2 dx \qquad (8.3)$$

The independent variables x and t are replaced by their non-dimensional counterparts:

$$\bar{x} = x/L \qquad ( )' = \frac{\partial}{\partial x}$$

$$\Psi = \Omega t \qquad (\,)^{\circ} = \frac{\partial}{\partial \Psi}$$

In addition, the following nondimensional quantities are defined:

$$\bar{\gamma} = \frac{\rho a c_{3/4}}{I_B} \qquad c_{3/4} = c_{x=\frac{3}{4}L}$$

$$\bar{c} = \frac{c}{c_{3/4}} \qquad \bar{c}_{3/4} = \frac{c_{3/4}}{L}$$

$$\bar{e}_x = \frac{e_x}{L} \qquad \bar{e}_Y = \frac{e_Y}{L} \tag{8.5}$$

$$\bar{e}_A = \frac{e_A}{L} \qquad \bar{e}_I = \frac{e_I}{L}$$

$$\bar{e}_T = \frac{e_T}{L} \qquad \bar{R}_T = \frac{R_T}{L}$$

$$\bar{k}_{m1} = \frac{k_{m1}}{L} \qquad \bar{k}_{m2} = \frac{k_{m2}}{L}$$

The assumed modes (Eqs. (8.1)) are also substituted into the expressions for T and $\dot{u}$ (Eqs. (7.3) and (7.6)), which are non-dimensionalized:

$$\frac{T}{\Omega^2 I_B/L} = \frac{(1-\beta_p^2)L^3}{I_B}\int_{\bar{x}}^{1} m\bar{x}\,d\bar{x} + \frac{\bar{e}_x L^3}{I_B}\int_{\bar{x}}^{1} m\,d\bar{x} + \frac{2L^3}{I_B}\int_{\bar{x}}^{1} m\gamma_v\,d\bar{x}\,\mathring{q}_v \tag{8.6}$$

$$\frac{\dot{u}}{L} = -\int_0^{\bar{x}} (\gamma_v')^2 d\bar{x}\, q_v \mathring{q}_v - \int_0^{\bar{x}} (\gamma_w')^2 d\bar{x}\, q_w \mathring{q}_w + \int_0^{\bar{x}} \bar{e}_T \cos\theta\, \gamma_v''\, d\bar{x}\, \mathring{q}_v + \int_0^{\bar{x}} \bar{e}_T \sin\theta\, \gamma_w''\, d\bar{x}\, \mathring{q}_w \tag{8.7}$$

A caution: some integrals must be integrated by parts to assure symmetry of the equations. The subsequent

application of the boundary conditions (Eqs. (8.2)) will eliminate all of the resulting boundary terms except one: $K_R \gamma_\phi^2(0)$. (This suggests the form of a modification to add a root spring about the y or z axis.)

Symbolically, the resulting equations are:

$$[M]\begin{Bmatrix}\ddot{q}_v\\ \ddot{q}_w\\ \ddot{q}_\phi\end{Bmatrix} + [C]\begin{Bmatrix}\dot{q}_v\\ \dot{q}_w\\ \dot{q}_\phi\end{Bmatrix} + [K]\begin{Bmatrix}q_v\\ q_w\\ q_\phi\end{Bmatrix} + \{P\}_{NL} = \{Q\} \tag{8.8}$$

These matrices will be defined later.

8.3 Static Equations

The aeroelastic stability must be studied for the blade displaced to its equilibrium position by the steady forces on it. Each generalized coordinate is separated into a static part and a small perturbation part, respectively:

$$\begin{aligned} q_v &= q_{vs} + \tilde{q}_v \\ q_w &= q_{ws} + \tilde{q}_w \\ q_\phi &= q_{\phi s} + \tilde{q}_\phi \end{aligned} \tag{8.9}$$

Then, the static parts may be found by solving the static equations:

$$[K]\begin{Bmatrix}q_v\\ q_w\\ q_\phi\end{Bmatrix} + \{P\}_{NL} = \{Q\} \tag{8.10}$$

8.4 Perturbation Equations

Substituting Eqs. (8.9) into the modal equations (Eqs. (8.8)), and ignoring all products of the perturbations yields the perturbation equations:

$$\left[M\right]\begin{Bmatrix}\ddot{q}_v\\ \ddot{q}_w\\ \ddot{q}_\phi\end{Bmatrix}+\left[C\right]\begin{Bmatrix}\dot{q}_v\\ \dot{q}_w\\ \dot{q}_\phi\end{Bmatrix}+\left[K+\Delta K\right]\begin{Bmatrix}q_v\\ q_w\\ q_\phi\end{Bmatrix}=\left\{0\right\} \tag{8.11}$$

The aeroelastic stability of the wind turbine blade is indicated by the complex eigenvalues of this system. Note that the ΔK matrix, and the C matrix, are functions of the static blade deflection.

8.5 Coefficient Integrals

The coefficients of the matrices of Eqs. (8.10) and Eqs. (8.11) are listed here:

$$\begin{aligned}K_{vv} = {} & \frac{1}{\Omega^2 I_\beta L}\int_0^1 (EI_2\cos^2\theta + EI_1\sin^2\theta)(\gamma_v'')^2\,d\bar{x}\\ & + \frac{(1-\beta_p^2)L^3}{I_\beta}\int_0^1 m\bar{x}\,\psi_v\,d\bar{x} + \bar{e}_x\frac{L^3}{I_\beta}\int_0^1 m\,\psi_v\,d\bar{x}\\ & - \frac{L^3}{I_\beta}\int_0^1 m\,\gamma_v^2\,d\bar{x}\end{aligned} \tag{8.12}$$

$$\begin{aligned}K_{vw} = {} & \frac{1}{\Omega^2 I_\beta L}\int_0^1 (EI_2 - EI_1)\sin\theta\cos\theta\,\gamma_w''\gamma_v''\,d\bar{x}\\ & - \frac{\bar{\delta}}{2}\int_0^1 \bar{c}\,\bar{e}_A\,\bar{x}^2\sin\theta\,\gamma_w'\gamma_v'\,d\bar{x}\end{aligned}$$

$$K_{v\phi} = \frac{-1}{\Omega^2 I_B L^2}\int_0^1 EB_2\,\theta'\cos\theta\,\gamma_\phi'\gamma_v''\,d\bar{x} + (1-\beta_p^2)\frac{L^3}{I_B}\int_0^1 m\bar{x}\,\Psi_{\phi v}\,d\bar{x}$$
$$+ \bar{e}_x\frac{L^3}{I_B}\int_0^1 m\,\Psi_{\phi v}\,d\bar{x} - \frac{L^3}{I_B}\int_0^1 m\bar{e}_I\bar{x}\sin\theta\,\gamma_\phi\gamma_v'\,d\bar{x}$$
$$+ \frac{L^3}{I_B}\int_0^1 m\bar{e}_I\sin\theta\,\gamma_\phi\gamma_v\,d\bar{x} + \frac{\bar{\gamma}}{2}\lambda\bar{R}_T\int_0^1\bar{c}\bar{x}\cos\theta\,\gamma_\phi\gamma_v\,d\bar{x}$$

$$K_{wv} = \frac{1}{\Omega^2 I_B L}\int_0^1 (EI_2 - EI_1)\sin\theta\cos\theta\,\gamma_w''\gamma_v''\,d\bar{x}$$
$$+ \frac{\bar{\gamma}}{2}\int_0^1\bar{c}\bar{e}_A\bar{x}^2\sin\theta\,\gamma_w'\gamma_v'\,d\bar{x} + \frac{\bar{\gamma}}{2}\beta_p\int_0^1\bar{c}\bar{x}\,\gamma_v\gamma_w\,d\bar{x}$$

$$K_{ww} = \frac{1}{\Omega^2 I_B L}\int_0^1 (EI_2\sin^2\theta + EI_1\cos^2\theta)(\gamma_w'')^2\,d\bar{x}$$
$$+ (1-\beta_p^2)\frac{L^3}{I_B}\int_0^1 m\bar{x}\,\Psi_w\,d\bar{x} + \bar{e}_x\frac{L^3}{I_B}\int_0^1 m\,\Psi_w\,d\bar{x}$$
$$+ \frac{\bar{\gamma}}{2}\bar{e}_Y\int_0^1\bar{c}\bar{x}\,\gamma_w'\gamma_w\,d\bar{x} - \frac{\bar{\gamma}}{2}\int_0^1\bar{c}\left[\bar{c}_{3/4}\left(\frac{\bar{c}}{2}+\frac{\bar{c}}{4}\cos\theta\right)-\bar{e}_A\right]\bar{x}\,\gamma_w'\gamma_w\,d\bar{x}$$

$$K_{wv} = \frac{1}{\Omega^2 I_B L}\int_0^1 (EI_2 - EI_1)\sin\theta\cos\theta\,\gamma_w''\gamma_v''\,d\bar{x}$$
$$+ \frac{\bar{\gamma}}{2}\int_0^1\bar{c}\bar{e}_A\bar{x}^2\sin\theta\,\gamma_w'\gamma_v'\,d\bar{x} + \frac{\bar{\gamma}}{2}\beta_p\int_0^1\bar{c}\bar{x}\,\gamma_v\gamma_w\,d\bar{x}$$

$$K_{w\phi} = \frac{-1}{\Omega^2 I_B L^2}\int_0^1 EB_2\,\theta'\sin\theta\,\gamma_\phi'\gamma_w''\,d\bar{x} - (1-\beta_p^2)\frac{L^3}{I_B}\int_0^1 m\bar{x}\,\Psi_{\phi w}\,d\bar{x}$$
$$- \bar{e}_x\frac{L^3}{I_B}\int_0^1 m\,\Psi_{\phi w}\,d\bar{x} + \frac{L^3}{I_B}\int_0^1 m\bar{e}_I\bar{x}\cos\theta\,\gamma_\phi\gamma_w'\,d\bar{x}$$
$$- \frac{\bar{\gamma}}{2}\int_0^1\bar{c}\bar{x}^2\cos\theta\,\gamma_\phi\gamma_w\,d\bar{x}$$

$$K_{\phi v} = \frac{-1}{\Omega^2 I_B L^2}\int_0^1 EB_2\,\theta'\cos\theta\,\gamma_\phi'\gamma_v''\,d\bar{x} + (1-\beta_p^2)\frac{L^3}{I_B}\int_0^1 m\bar{x}\,\Psi_{\phi v}\,d\bar{x}$$
$$+\bar{e}_x\frac{L^3}{I_B}\int_0^1 m\,\Psi_{\phi v}\,d\bar{x} - \frac{L^3}{I_B}\int_0^1 m\bar{e}_I\,\bar{x}\,\sin\theta\,\gamma_\phi\,\gamma_v'\,d\bar{x}$$
$$+\frac{L^3}{I_B}\int_0^1 m\bar{e}_I\sin\theta\,\gamma_\phi\,\gamma_v\,d\bar{x}$$

$$K_{\phi w} = \frac{-1}{\Omega^2 I_B L^2}\int_0^1 EB_2\,\theta'\sin\theta\,\gamma_\phi'\gamma_w''\,d\bar{x} - (1-\beta_p^2)\frac{L^3}{I_B}\int_0^1 m\bar{x}\,\Psi_{\phi w}\,d\bar{x}$$
$$-\bar{e}_x\frac{L^3}{I_B}\int_0^1 m\,\Psi_{\phi w}\,d\bar{x} + \frac{L^3}{I_B}\int_0^1 m\bar{e}_I\,\bar{x}\cos\theta\,\gamma_\phi\,\gamma_w'\,d\bar{x}$$

$$K_{\phi\phi} = \frac{K_R}{\Omega^2 I_B}\gamma_{\phi_R}^2 + \frac{1}{\Omega^2 I_B L}\int_0^1 GJ_E\,(\gamma_\phi')^2\,d\bar{x} + \frac{L^3}{I_B}\int_0^1 m\bar{x}\,\Psi_\phi\,d\bar{x}$$
$$+\frac{L^3}{I_B}\int_0^1 m\,(k_{m2}^2 - k_{m1}^2)(\cos^2\theta - \sin^2\theta)\,\gamma_\phi^2\,d\bar{x}$$

$$\Delta K_{vv} = \frac{-2}{\Omega^2 I_B L}\int_0^1 (EI_2 - EI_1)\sin\theta\cos\theta\,\gamma_\phi\,(\gamma_v'')^2\,d\bar{x}\;\;q_{\phi s}$$

$$\Delta K_{vw} = \frac{1}{\Omega^2 I_B L}\int_0^1 (EI_2 - EI_1)(\cos^2\theta - \sin^2\theta)\,\gamma_\phi\,\gamma_w''\gamma_v''\,d\bar{x}\;\;q_{\phi s}$$

$$\Delta K_{v\phi} = \frac{-2}{\Omega^2 I_B L}\int_0^1 (EI_2 - EI_1)\sin\theta\cos\theta\,\gamma_\phi\,(\gamma_v'')^2\,d\bar{x}\;\;q_{vs}$$
$$+\frac{1}{\Omega^2 I_B L}\int_0^1 (EI_2 - EI_1)(\cos^2\theta - \sin^2\theta)\,\gamma_\phi\,\gamma_w''\gamma_v''\,d\bar{x}\;\;q_{ws}$$

$$\Delta K_{wv} = \frac{1}{\Omega^2 I_B L}\int_0^1 (EI_2 - EI_1)(\cos^2\theta - \sin^2\theta)\,\gamma_\phi\,\gamma_w''\gamma_v''\,d\bar{x}\;q_{\phi s} + \frac{\bar{\gamma}}{2}\int_0^1 \bar{c}\,\bar{x}\,\gamma_w'\,\gamma_{w1}\,\gamma_v\,d\bar{x}\;q_{ws}$$

$$\Delta K_{ww} = \frac{2}{\Omega^2 I_B L}\int_0^1 (EI_2 - EI_1)\sin\theta\cos\theta\,\gamma_\phi\,(\gamma_w'')^2\,d\bar{x}\;q_{\phi s} + \frac{\bar{\gamma}}{2}\int_0^1 \bar{c}\,\bar{x}\,\gamma_w'\,\gamma_w\,\gamma_v\,d\bar{x}\;q_{vs}$$

$$\Delta K_{w\phi} = \frac{1}{\Omega^2 I_B L}\int_0^1 (EI_2 - EI_1)(\cos^2\theta - \sin^2\theta)\,\gamma_\phi\,\gamma_w''\gamma_v''\,d\bar{x}\;q_{vs} + \frac{2}{\Omega^2 I_B L}\int_0^1 (EI_2 - EI_1)\sin\theta\cos\theta\,\gamma_\phi\,(\gamma_w'')^2\,d\bar{x}\;q_{ws}$$

$$\Delta K_{\phi v} = \Delta K_{v\phi}$$

$$\Delta K_{\phi w} = \Delta K_{w\phi}$$

$$\Delta K_{\phi\phi} = 0$$

$$C_{vv} = 2\frac{L^3}{I_B}\int_0^1 m\,\gamma_v\,\psi_{\phi v}\,d\bar{x}\;q_{\phi_s} + \frac{\bar{\gamma}}{2}\lambda\bar{R}_T\int_0^1 \bar{c}\,\sin\theta\,\gamma_v^2\,d\bar{x} + \bar{\gamma}\,\frac{C_{D_0}}{a}\int_0^1 \bar{c}\,\bar{x}\,\gamma_v^2\,d\bar{x}$$

$$C_{vw} = -2\frac{L^3}{I_B}\int_0^1 m\,\gamma_v\,\psi_w\,d\bar{x}\;q_{w_s} + 2\frac{L^3}{I_B}\int_0^1 m\,\gamma_v\,\psi_{wv}\,d\bar{x} - 2\beta_p\frac{L^3}{I_B}\int_0^1 m\,\gamma_w\gamma_v\,d\bar{x} - 2\frac{L^3}{I_B}\int_0^1 m\,\bar{e}_I\,\sin\theta\,\gamma_w'\gamma_v\,d\bar{x} + \frac{\bar{\gamma}}{2}\int_0^1 \bar{c}\,\bar{x}\,\sin\theta\,\gamma_w\gamma_v\,d\bar{x} - \frac{\bar{\gamma}}{2}\lambda\bar{R}_T\int_0^1 \bar{c}\,(1+\cos\theta)\,\gamma_w\gamma_v\,d\bar{x}$$

$$C_{v\phi} = 0$$

$$C_{wv} = -2\frac{L^3}{I_B}\int_0^1 m\,\gamma_v\,\psi_{\phi w}\,d\bar{x}\;q_{\phi_s} + 2\frac{L^3}{I_B}\int_0^1 m\,\gamma_v\,\psi_w\,d\bar{x}\;q_{w_s} - 2\frac{L^3}{I_B}\int_0^1 m\,\gamma_v\,\psi_{we}\,d\bar{x} + 2\beta_p\frac{L^3}{I_B}\int_0^1 m\,\gamma_w\gamma_v\,d\bar{x} + 2\frac{L^3}{I_B}\int_0^1 m\,\bar{e}_I\,\sin\theta\,\gamma_w'\gamma_v\,d\bar{x} - \bar{\gamma}\int_0^1 \bar{c}\,\bar{x}\,\sin\theta\,\gamma_w\,\gamma_v\,d\bar{x} + \frac{\bar{\gamma}}{2}\lambda\bar{R}_T\int_0^1 \bar{c}\,(2\cos\theta-1)\,\gamma_v\gamma_w\,d\bar{x}$$

$$C_{ww} = \frac{\bar{\gamma}}{2}\int_0^1 \bar{c}\,\bar{x}\,\gamma_w^2\,d\bar{x} - \frac{\bar{\gamma}}{2}\lambda\bar{R}_T\int_0^1 \bar{c}\,\sin\theta\,\gamma_w^2\,d\bar{x}$$

$$C_{w\phi} = -\frac{\bar{\gamma}}{2}\int_0^1 \bar{c}\left[\bar{c}_{3/4}\left(\frac{\bar{c}}{2}+\frac{\bar{c}}{4}\cos\theta\right)-\bar{e}_A\right]\bar{x}\,\gamma_\phi\,\gamma_w\,d\bar{x}$$

$$C_{\phi v} = -\bar{\gamma}\int_0^1 \bar{c}\,\bar{e}_A\,\bar{x}\,\sin\theta\;\gamma_v\,\gamma_\phi\,d\bar{x}$$

$$+2\frac{L^3}{I_B}\int_0^1 m\,\gamma_v\,\psi_{\phi v}\,d\bar{x}\,q_{vs}-2\frac{L^3}{I_B}\int_0^1 m\,\gamma_v\,\psi_{\phi w}\,d\bar{x}\,q_{ws}$$

$$C_{\phi w} = \frac{\bar{\gamma}}{2}\int_0^1 \bar{c}\,\bar{e}_A\,\bar{x}\,\gamma_w\,\gamma_\phi\,d\bar{x}$$

$$C_{\phi\phi} = \frac{\bar{\gamma}}{2}\int_0^1 \bar{c}\left(\bar{c}_{3/4}\frac{\bar{c}}{4}-\bar{e}_A\right)\left(\bar{c}_{3/4}\frac{\bar{c}}{2}-e_A\right)\bar{x}\,\gamma_\phi^{\,2}\,d\bar{x}$$

$$M_{rr} = \frac{L^3}{I_B}\int_0^1 m\,\gamma_r^2\,d\bar{x} + \frac{\bar{\gamma}}{8}\int_0^1 \bar{c}^2\bar{c}_{3/4}\,\sin^2\theta\,\gamma_r^2\,d\bar{x}$$

$$M_{rw} = -\frac{\bar{\gamma}}{8}\int_0^1 \bar{c}^2\bar{c}_{3/4}\,\sin\theta\,\gamma_w\,\gamma_r\,d\bar{x}$$

$$M_{r\phi} = -\frac{L^3}{I_B}\int_0^1 m\bar{e}_I\,\sin\theta\,\gamma_\phi\,\gamma_r\,d\bar{x}$$

$$M_{wr} = -\frac{\bar{\gamma}}{8}\int_0^1 \bar{c}^2\bar{c}_{3/4}\,\sin\theta\cos\theta\,\gamma_r\,\gamma_w\,d\bar{x}$$

$$M_{ww} = \frac{L^3}{I_B}\int_0^1 m\,\gamma_w^2\,d\bar{x} + \frac{\bar{\gamma}}{8}\int_0^1 \bar{c}^2\bar{c}_{3/4}\cos\theta\,\gamma_w^2\,d\bar{x}$$

$$M_{w\phi} = \frac{L^3}{I_B}\int_0^1 m\bar{e}_I\cos\theta\,\gamma_\phi\,\gamma_w\,d\bar{x}$$

$$M_{\phi r} = M_{r\phi}$$

$$M_{\phi w} = M_{w\phi}$$

$$M_{\phi\phi} = \frac{L^3}{I_B}\int_0^1 m\,(\bar{k}_{m_2}^2 + \bar{k}_{m_1}^2)\,\gamma_\phi^2\,d\bar{x}$$

$$P_v = -\frac{2}{\Omega^2 I_B L}\int_0 (EI_2 - EI_1)\sin\theta\cos\theta\ \gamma_\phi(\gamma_v'')^2 d\bar{x}\ q_{\phi_s} q_{v_s}$$

$$+\frac{1}{\Omega^2 I_B L}\int_0^1 (EI_2 - EI_1)(\cos^2\theta - \sin^2\theta)\gamma_\phi \gamma_w'' \gamma_v'' d\bar{x}\ q_{\phi_s} q_{w_s}$$

$$P_w = \frac{1}{\Omega^2 I_B L}\int_0 (EI_2 - EI_1)(\cos^2\theta - \sin^2\theta)\gamma_\phi \gamma_w'' \gamma_v'' d\bar{x}\ q_{\phi_s} q_{v_s}$$

$$+\frac{2}{\Omega^2 I_B L}\int_0^1 (EI_2 - EI_1)\sin\theta\cos\theta\ \gamma_\phi(\gamma_w'')^2 d\bar{x}\ q_{\phi_s} q_{w_s}$$

$$+\frac{\bar{\gamma}}{2}\int_0^1 \bar{c}\,\bar{x}\,\gamma_w'\gamma_w\gamma_v\, d\bar{x}\ q_{r_s} q_{w_s}$$

$$P_\phi = \frac{-1}{\Omega^2 I_B L}\int_0^1 (EI_2 - EI_1)\sin\theta\cos\theta\ \gamma_\phi(\gamma_v'')^2 d\bar{x}\ q_{v_s}^2$$

$$+\frac{1}{\Omega^2 I_B L}\int_0^1 (EI_2 - EI_1)(\cos^2\theta - \sin^2\theta)\gamma_\phi \gamma_w'' \gamma_v'' d\bar{x}\ q_{r_s} q_{w_s}$$

$$+\frac{1}{\Omega^2 I_B L}\int_0^1 (EI_2 - EI_1)\sin\theta\cos\theta\ \gamma_\phi(\gamma_w'')^2 d\bar{x}\ q_{w_s}^2$$

$$Q_v = -\frac{L^3}{I_B}\int_0^1 m\bar{e}_I\bar{x}\cos\theta\,\gamma_v'\,d\bar{x} - \bar{e}_x\frac{L^3}{I_B}\int_0^1 m\bar{e}_I\cos\theta\,\gamma_v'\,d\bar{x}$$
$$+\bar{e}_y\frac{L^3}{I_B}\int_0^1 m\gamma_v\,d\bar{x} + \frac{L^3}{I_B}\int_0^1 m\bar{e}_I\cos\theta\,\gamma_v\,d\bar{x}$$
$$+\frac{\bar{\gamma}}{2}\lambda^2\bar{R}_T^2\int_0^1\bar{c}\cos\theta\,\gamma_v\,d\bar{x} - \frac{\bar{\gamma}}{2}\lambda\bar{R}_T(1-\beta_p^2)\int_0^1\bar{c}\bar{x}\sin\theta\,\gamma_v\,d\bar{x}$$
$$-\frac{\bar{\gamma}}{2}\lambda\bar{R}_T\bar{e}_x\int_0^1\bar{c}\sin\theta\,\gamma_v\,d\bar{x} - \frac{\bar{\gamma}}{2}\frac{C_{Do}}{a}\int_0^1\bar{c}\bar{x}^2\gamma_v\,d\bar{x}$$
$$+(1-\beta_p^2)\frac{L^3}{I_B}\int_0^1 m\bar{x}\,\psi_{ve}\,d\bar{x} + \bar{e}_x\frac{L^3}{I_B}\int_0^1 m\,\psi_{ve}\,d\bar{x}$$

$$Q_w = -\frac{L^3}{I_B}\int_0^1 m\bar{e}_I\bar{x}\sin\theta\,\gamma_w'\,d\bar{x} - \bar{e}_x\frac{L^3}{I_B}\int_0^1 m\bar{e}_I\sin\theta\,\gamma_w'\,d\bar{x}$$
$$-\beta_p\frac{L^3}{I_B}\int_0^1 m\bar{x}\,\gamma_w\,d\bar{x} - \beta_p\bar{e}_x\frac{L^3}{I_B}\int_0^1 m\gamma_w\,d\bar{x}$$
$$+\frac{\bar{\gamma}}{2}(1-\beta_p^2)\int_0^1\bar{c}\bar{x}^2\sin\theta\,\gamma_w\,d\bar{x} + \bar{\gamma}\bar{e}_x\int_0^1\bar{c}\bar{x}\sin\theta\,\gamma_w\,d\bar{x}$$
$$-\frac{\bar{\gamma}}{2}\lambda\bar{R}_T\int_0^1\bar{c}\bar{x}\cos\theta\,\gamma_w\,d\bar{x} - \frac{\bar{\gamma}}{2}\lambda\bar{R}_T\bar{e}_x\int_0^1\bar{c}\cos\theta\gamma_w\,d\bar{x}$$
$$-\frac{\bar{\gamma}}{2}\beta_p\bar{e}_y\int_0^1\bar{c}\bar{x}\,\gamma_w\,d\bar{x} + \frac{\bar{\gamma}}{2}\beta_p\int_0^1\bar{c}\bar{x}\left[\bar{c}_{3/4}\left(\frac{\bar{c}}{2}+\frac{\bar{c}}{4}\cos\theta\right)-\bar{e}_A\right]\gamma_w\,d\bar{x}$$
$$+(1-\beta_p^2)\frac{L^3}{I_B}\int_0^1 m\bar{x}\,\psi_{we}\,d\bar{x} + \bar{e}_x\frac{L^3}{I_B}\int_0^1 m\,\psi_{we}\,d\bar{x}$$

$$Q_\phi = -(1-\beta_p^2)\frac{L^3}{I_B}\int_0^1 m\bar{x}\,\Psi_{\theta\phi}\,d\bar{x} - \bar{e}_x\frac{L^3}{I_B}\int_0^1 m\,\Psi_{\theta\phi}\,d\bar{x}$$

$$-\beta_p\frac{L^3}{I_B}\int_0^1 m\bar{e}_I\bar{x}\cos\theta\,\gamma_\phi\,d\bar{x} - \bar{e}_Y\frac{L^3}{I_B}\int_0^1 m\bar{e}_I\sin\theta\,\gamma_\phi\,d\bar{x}$$

$$-\frac{L^3}{I_B}\int_0^1 m(\bar{k}_{m2}^2-\bar{k}_{m1}^2)\sin\theta\cos\theta\,\gamma_\phi\,d\bar{x}$$

$$+\frac{\bar{\gamma}}{2}(1-\beta_p^2)\int_0^1 \bar{c}\,\bar{e}_A\,\bar{x}^2\sin\theta\,\gamma_\phi\,d\bar{x} + \bar{\gamma}\bar{e}_x\int_0^1 \bar{c}\,\bar{e}_A\bar{x}\sin\theta\gamma_\phi\,d\bar{x}$$

$$-\frac{\bar{\gamma}}{2}\lambda\bar{R}_T\int_0^1 \bar{c}\,\bar{e}_A\bar{x}\cos\theta\,\gamma_\phi\,d\bar{x} + \frac{\bar{\gamma}}{4}\lambda^2\bar{R}^2\int_0^1 \bar{c}\,\bar{e}_A\cos\theta\,\gamma_\phi\,d\bar{x}$$

where:

$$\Psi_v = \int_0^{\bar{x}}(\gamma_v')^2\,d\bar{x}$$

$$\Psi_w = \int_0^{\bar{x}}(\gamma_w')^2\,d\bar{x}$$

$$\Psi_\phi = \int_0^{\bar{x}} k_A^2\,\theta'\gamma_\phi'\,d\bar{x}$$

$$\Psi_{\phi v} = \int_0^{\bar{x}}\bar{e}_T\sin\theta\,\gamma_\phi\,\gamma_v''\,d\bar{x}$$

$$\Psi_{\phi w} = \int_0^{\bar{x}}\bar{e}_T\cos\theta\,\gamma_\phi\,\gamma_w''\,d\bar{x}$$

$$\Psi_{ve} = \int_0^{\bar{x}}\bar{e}_T\cos\theta\,\gamma_v''\,d\bar{x}$$

$$\Psi_{we} = \int_0^{\bar{x}}\bar{e}_T\sin\theta\,\gamma_w''\,d\bar{x}$$

Chapter IX

Sample Solution: The NASA-ERDA 100-kw Wind Turbine

The modal equations of Chapter 8 have been solved for the NASA-ERDA 100 kw Wind Turbine. The purpose of generating this solution was to verify results computed using the equivalent hinge model developed for the Wind Energy Conversion Project.[1] Numerical comparisons are documented here, as well as a term by term comparison of the two systems of equations.

The equivalent hinge model represents the blade as a rigid rod with springs at the root about the axes. This allows the blade three angular degrees of freedom, corresponding to the three generalized coordinates of the present analysis (see Fig. 9.4). The rotating natural frequencies of the spring-rod system are matched to those of the blade under study (see Appendix 2B).

9.1 Mode Shapes and Natural Frequencies

The mode shapes γ_v and γ_w, and the frequencies ω_v and ω_w were taken from Donham, Schmidt, and Linscott.[5] The mode shape γ_ϕ and the frequency ω_ϕ were calculated using a simple iterative scheme. All numerical values are tabulated in Appendix 2A, for 10 spanwise stations.

The required derivatives were calculated using three point finite difference operators of the central difference type. As with the equivalent hinge model, the resulting non-rotating, uncoupled natural frequencies must match those of the actual blade. The derivatives γ_v'', γ_w'', and γ_ϕ' were corrected by multiplicative factors so that:

$$\omega_v^2 = \frac{\int_0^1 EI_2(\gamma_v'')^2 d\bar{x}}{L^4 \int_0^1 m \gamma_v^2 d\bar{x}}$$

$$\omega_w^2 = \frac{\int_0^1 EI_1(\gamma_w'')^2 d\bar{x}}{L^4 \int_0^1 m \gamma_v^2 d\bar{x}} \qquad (9.1)$$

$$\omega_\phi^2 = \frac{K_R \gamma_{\phi_R}^2 + \frac{1}{L}\int_0^1 GJ_e(\gamma_\phi')^2 d\bar{x}}{L^3 \int_0^1 m \bar{k}_m^2 \gamma_\phi^2 d\bar{x}}$$

9.2 Solution Process

The integrals of Section 8.5 were calculated using the trapezoidal rule for numerical integration. It was found that a linear solution was adequate for the static displacements, so the P matrix was ignored in Eq. (8.10). A FORTRAN program was written which solves the static equations, sets up the perturbation equations using the static solution, and extracts the eigenvalues, using the EISPAC subroutine package (Argonne National Laboratory).

The program was used to calculate the rotating modes and frequencies with no air loads. The calculated modal coupling and frequencies are in excellent agreement to those documented by Donham, Schmidt, and Linscott,[5] as shown by Table 9.1.

	Flap Mode		Lag Mode	
	$\frac{\omega_w}{\Omega}$	$\frac{q_r}{q_w}\Big\|_{\bar{x}=\frac{3}{4}}$	$\frac{\omega_r}{\Omega}$	$\frac{q_w}{q_r}\Big\|_{\bar{x}=\frac{3}{4}}$
Present Analysis:	2.77	.172	3.61	.174
Reference 5:	2.76	.166	3.62	.169

Table 9.1

9.3 Equivalent Hinge Comparison: Numerical

The present program was used in conjunction with an existing equivalent hinge program to generate three graphic comparisons. Figure 9.1 compares two plots of lag mode damping versus torsion frequency ratio for various values of precone angle. Although the comparison for $\beta_p = -.24$ is poor, the results are generally in good agreement qualitatively, including the stability boundaries. Here, the

FIGURE 9.1 LAG MODE DAMPING VS. TORSION FREQUENCY RATIO

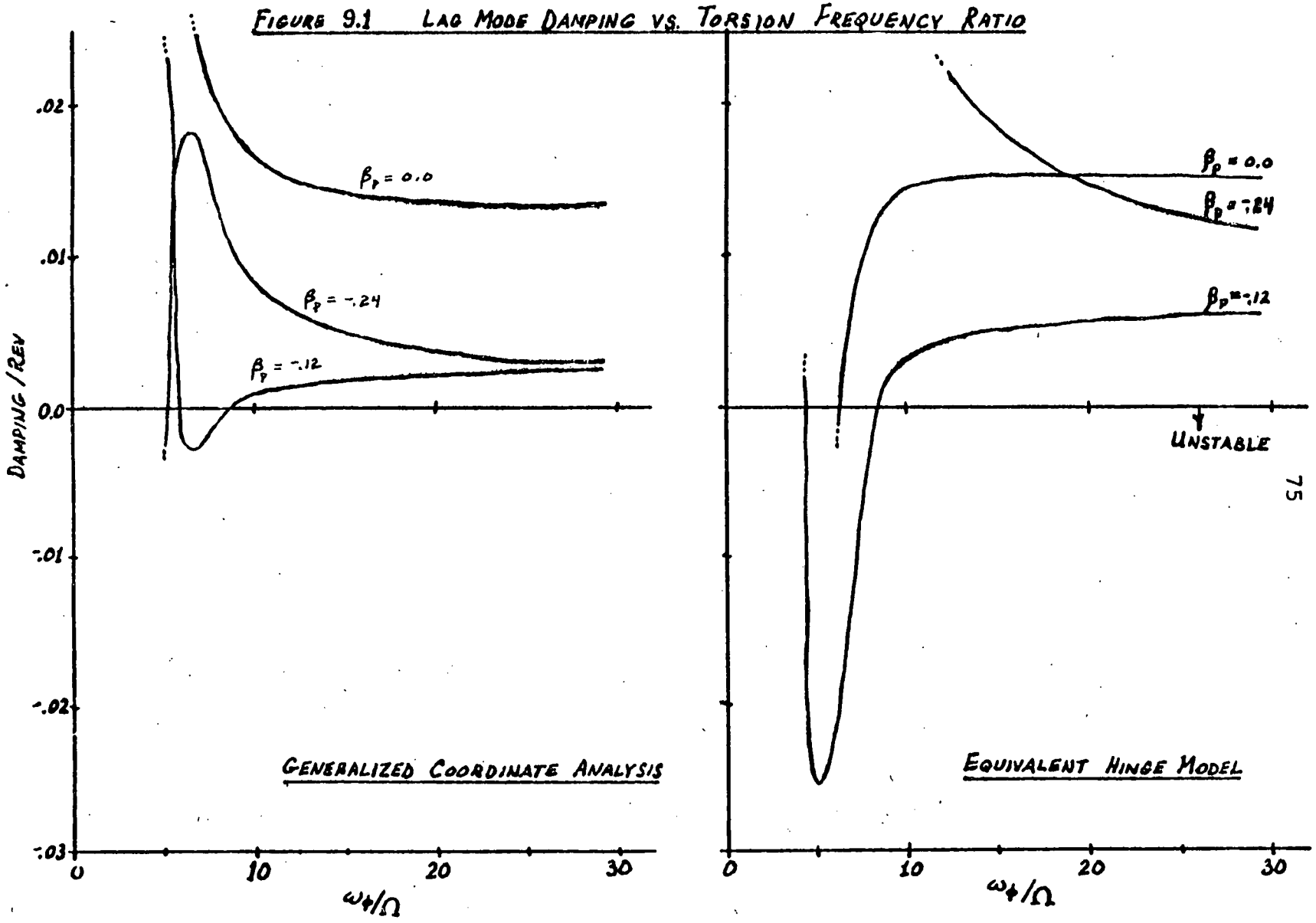

FIGURE 9.2 LAG MODE DAMPING VS INDUCED INFLOW ANGLE

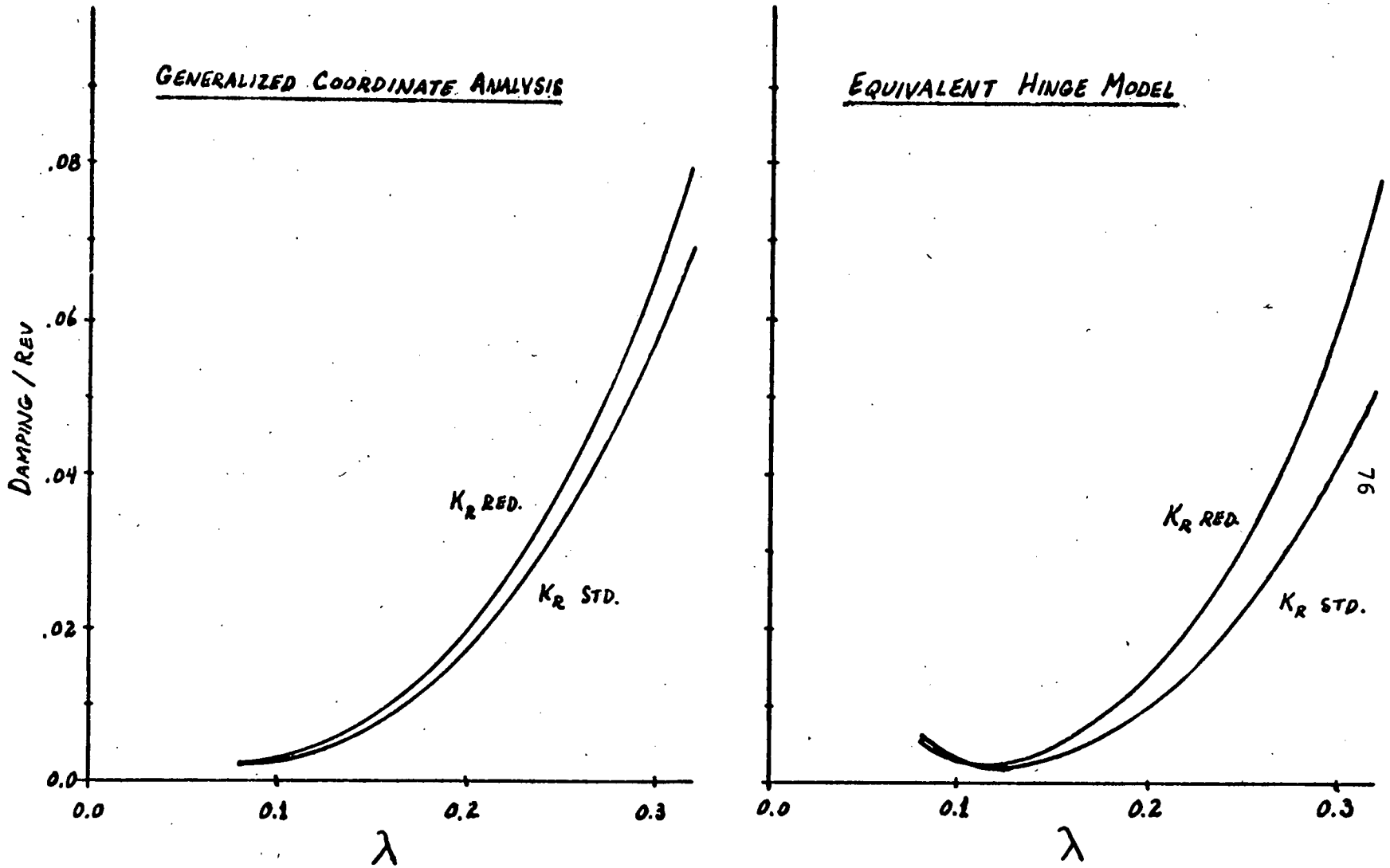

FIG. 9.2 CONT. LAG MODE DAMPING VS. INFLOW ANGLE λ

$\beta_p = -.12$

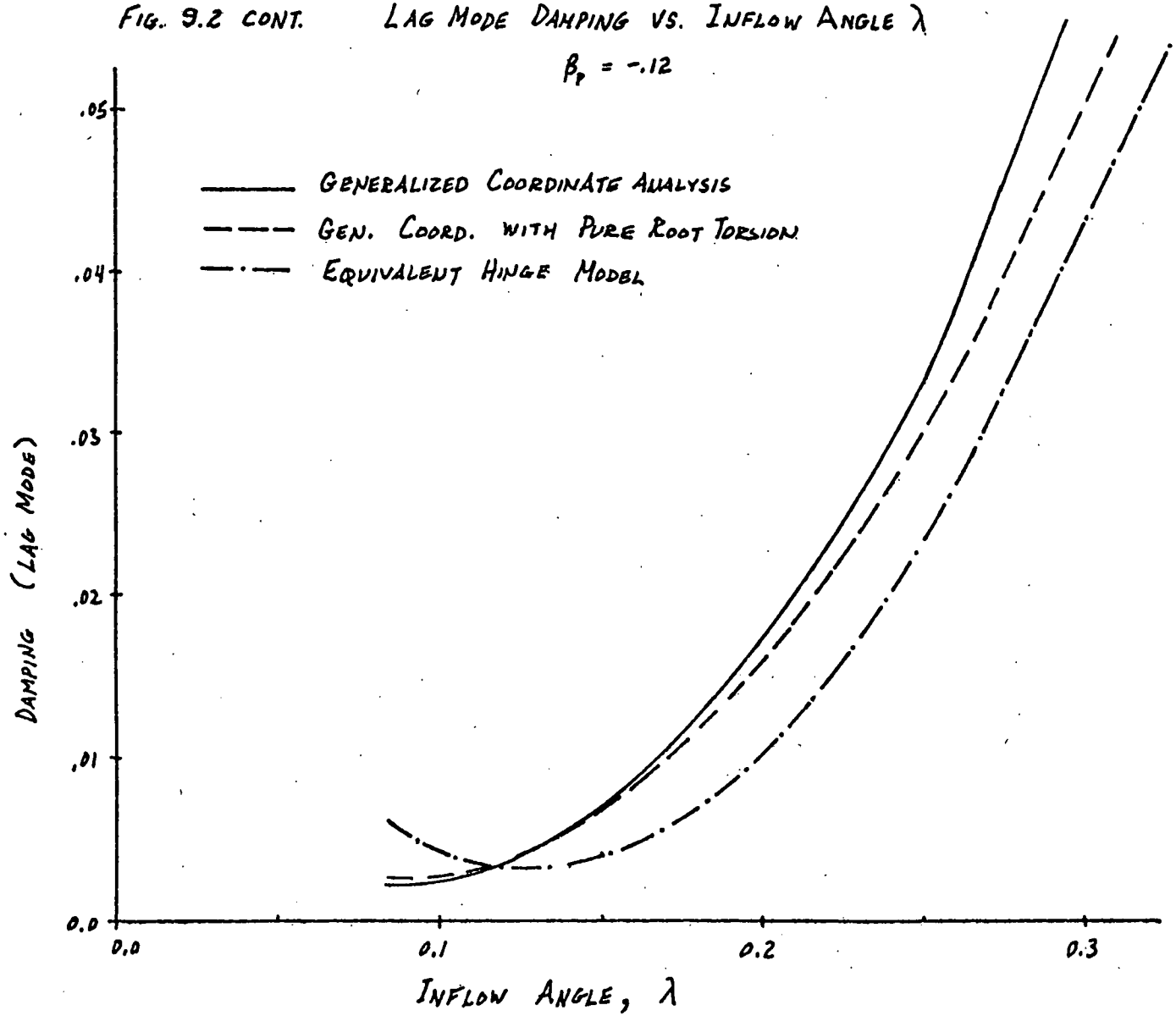

FIGURE 9.3 LAG MODE DAMPING VS PRECONE ANGLE

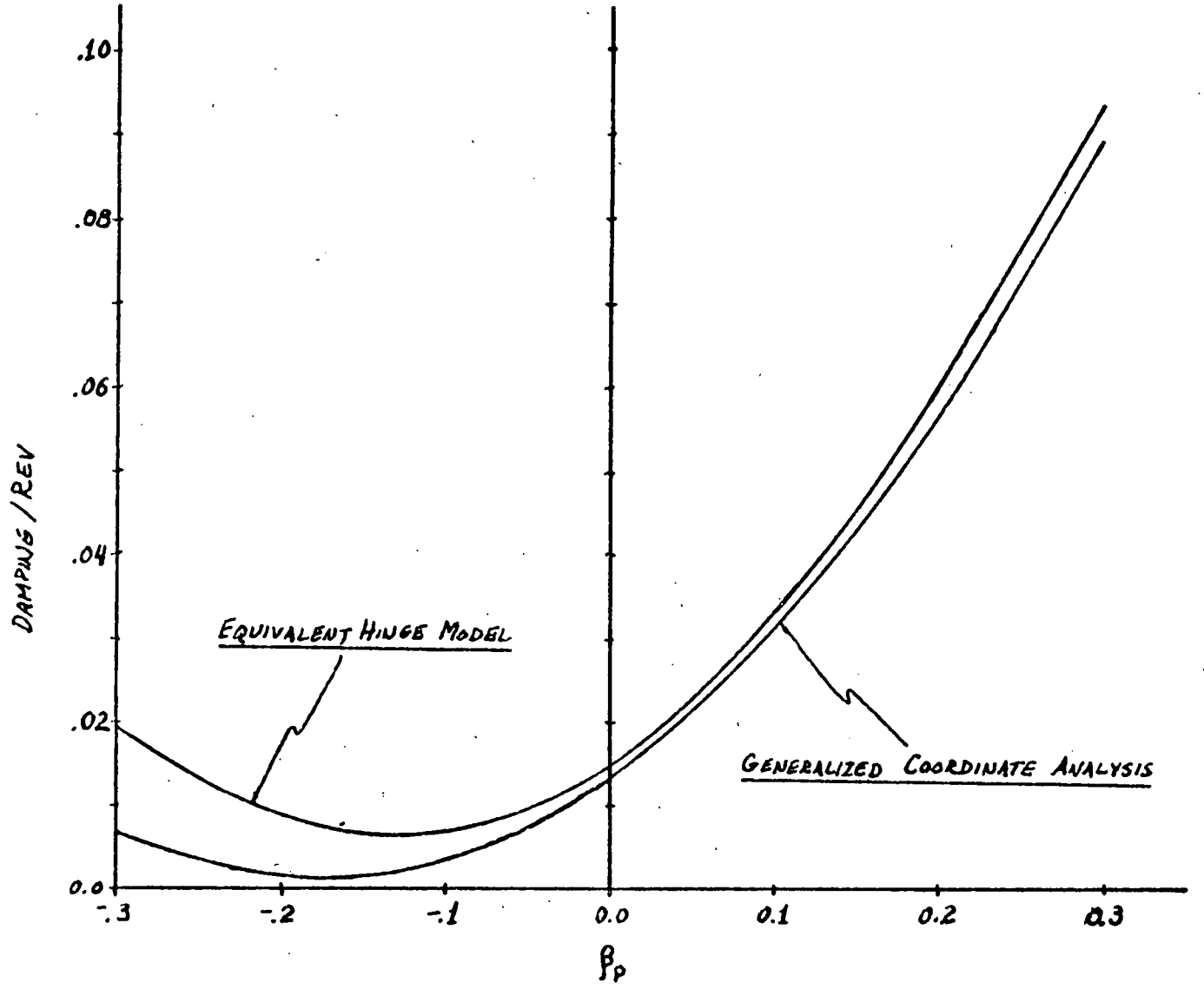

torsion frequency is reduced by reducing the control system stiffness.

Figure 9.2 compares two plots of lag mode damping versus induced inflow angle for the standard control system and one half as stiff. Again the behavior is very comparable. Figure 9.3 compares the two models in a plot of lag mode damping versus precone angle. In all of these plots, the lag mode is singled out because it is the most sensitive.

Figure 9.2 also illustrates the aeroelastic stability of the NASA-ERDA 100 kw wind turbine in its standard configuration, for K_R standard.[6] The λ variation corresponds to a wind speed of 10 mph gusting to 60 mph.

9.4 Equivalent Hinge Comparison: Term by Term

The form of the equivalent hinge equations is:

$$[M_E]\begin{Bmatrix}\ddot{\beta}_E\\ \ddot{\phi}_E\\ \ddot{\theta}_E\end{Bmatrix} + [C_E]\begin{Bmatrix}\dot{\beta}_E\\ \dot{\phi}_E\\ \dot{\theta}_E\end{Bmatrix} + [K_E]\begin{Bmatrix}\beta_E\\ \phi_E\\ \theta_E\end{Bmatrix} = \{0\} \qquad (9.2)$$

Although the equivalent hinge coordinates represent blade motions comparable to the generalized coordinates of this study, they are fundamentally different. The equivalent hinge coordinates are angles measured from the root as shown by Fig. 9.4, which compares the two systems.

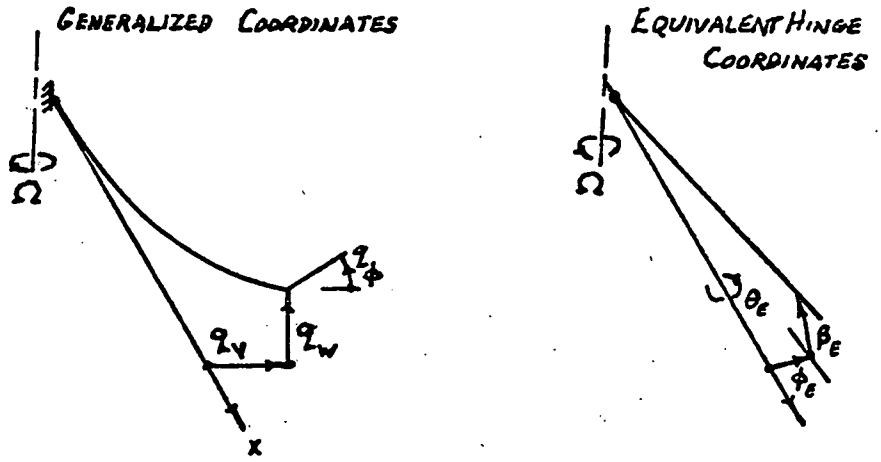

Fig. 9.4

The matrix coefficients used in the equivalent hinge equations are listed in Appendix III. A detailed comparison with the coefficient integrals of Section 8.5 has been completed with simple mode shapes and parameters. There are two major results of this term by term comparison: First, All of the important terms and effects compare extremely well; Second, Because of the different coordinate systems, the equivalent hinge model has some inertia coupling terms with no counterparts in the present model. The generalized coordinate model has similar stiffness coupling terms with no counterparts.

Chapter X

CONCLUSIONS

The nonlinear equations of motion of a general wind turbine blade have been derived. Understanding the source of the various terms in these equations is a key to understanding the dynamic problems associated with wind turbine design. The equations, with suitable boundary conditions, are applicable to many horizontal axis wind turbines presently conceived or operating, and provides a foundation for further study of wind turbine blade dynamics.

A sample numerical solution has been completed to study the aeroelastic stability of the NASA-ERDA 100 kw wind turbine. The modal equations developed are applicable to similar wind turbines if suitable Galerkin modes are used to calculate the coefficient integrals. This generalized coordinate analysis has been compared to an equivalent hinge model used in "Wind Energy Conversion".[1] The two solutions have been compared for a limited variation of the most important parameters, and the equations of motion themselves have been scrutinized.

The NASA machine is a demanding test for several reasons, which may not apply to other machines. Some angles are too large for the small angle assumption used in the equivalent hinge model. This is demonstrated by the

increasing difference between the two calculations as λ or β_p increase in Figs. 9.2 and 9.3, and the poor results for $\beta_p = -.24$ noted earlier.

The NASA wind turbine exhibits a remarkable distribution of flexibility in its bending mode shapes, and considerable distributed torsion. Quite naturally, the equivalent hinge model demonstrates better accuracy for blades where most of the flexure is in the root area. Marked improvement was noted after simply eliminating the distributed torsion in favor of purely root torsion. Excellent results may be expected for systems with articulated or flexible strap hubs.

It was also discovered that the rotating natural frequencies should be matched when specifying frequencies for the equivalent hinge model, rather than the nonrotating frequencies. Again this was because of the highly distributed bending of the NASA machine.

If the limitations of the equivalent hinge model are observed, it is adequate for its intended use as a preliminary design tool. The model represents all of the important effects well, and produces excellent qualitative results. For some systems, the simple equivalent hinge model gives good quantitative results as well, and may be the only aeroelastic stability analysis needed.

Appendix I

Coordinate Transformations

The rotation from xyz to XYZ is β_p about y, so that:

$$\begin{Bmatrix} \hat{I} \\ \hat{J} \\ \hat{K} \end{Bmatrix} = \begin{bmatrix} \cos\beta_p & 0 & -\sin\beta_p \\ 0 & 1 & \\ \sin\beta_p & 0 & \cos\beta_p \end{bmatrix} \begin{Bmatrix} \hat{i} \\ \hat{j} \\ \hat{k} \end{Bmatrix} \tag{A1}$$

Note that later, use is made of the approximations:

$$\sin\beta_p \cong \beta_p \qquad \cos\beta_p \cong 1 - \tfrac{1}{2}\beta_p^2 \tag{A2}$$

For now, the present form of A1 is most convenient.

The rotations from xyz to $x_2y_2z_2$ are $\tan^{-1}v'$ about z and $\tan^{-1}w'$ about y. Using the approximations:

$$\begin{aligned} \sin\measuredangle_z &\cong v' & \cos\measuredangle_z &\cong 1 - \tfrac{1}{2}v'^2 \\ \sin\measuredangle_y &\cong w' & \cos\measuredangle_y &\cong 1 - \tfrac{1}{2}w'^2 \end{aligned} \tag{A3}$$

$$\begin{Bmatrix} \hat{i}_2 \\ \hat{j}_2 \\ \hat{k}_2 \end{Bmatrix} = \begin{bmatrix} 1 - \frac{1}{2}v'^2 - \frac{1}{2}w'^2 & v' & w' \\ -v' & 1 - \frac{1}{2}v'^2 & 0 \\ -w' & -v'w' & 1 - \frac{1}{2}w'^2 \end{bmatrix} \begin{Bmatrix} \hat{i} \\ \hat{j} \\ \hat{k} \end{Bmatrix} \tag{A4}$$

Finally, the rotation from $x_2y_2z_2$ to $\xi\eta\zeta$ is approximately $\theta + \phi$ about x_2. Multiplying this rotation into Eq. (A4) gives:

$$\begin{Bmatrix} \hat{i}_\xi \\ \hat{i}_\eta \\ \hat{i}_\zeta \end{Bmatrix} = \begin{bmatrix} 1-\frac{1}{2}v'^2-\frac{1}{2}w'^2 & v' & w' \\ -(v'\cos(\theta+\phi)+w'\sin(\theta+\phi)) & \cos(\theta+\phi) & \sin(\theta+\phi) \\ -(w'\cos(\theta+\phi)-v'\sin(\theta+\phi)) & -\sin(\theta+\phi) & \cos(\theta+\phi) \end{bmatrix} \begin{Bmatrix} \hat{i} \\ \hat{j} \\ \hat{k} \end{Bmatrix} \tag{A5}$$

Again, this form is most convenient now, but later the following expansions are used:

$$\begin{aligned} \sin(\theta+\phi) &\cong \sin\theta + \phi\cos\theta \\ \cos(\theta+\phi) &\cong \cos\theta - \phi\sin\theta \end{aligned} \tag{A6}$$

Appendix II

NASA-ERDA 100 kw Wind Turbine Data

A. Generalized Coordinate Model

B. Equivalent Hinge Model

2A. Generalized Coordinate Model

The various non-dimensional parameters are given in Tables A1 and A2, as distilled from Ref. 5.

TABLE A1

$\bar{\gamma} = 11.218$

$\bar{R}_T = 1.0368$

$\bar{e}_x = .04394$

$\bar{e}_y = 0$

$\bar{c}_{3/4} = .04123$

$\bar{e}_A \cong 0$

$\bar{e}_T \cong 0$

$L = 59.85$ ft.

$\Omega = 40$ rpm $= 4.19 \frac{rad}{sec}$

$\beta_p = -7^\circ = -.12$ rad

$a = 6$

$c_{d_0} = .012$

$\rho = .00238 \frac{sl}{ft^3}$

$K_\beta = 405,850 \frac{ft\text{-}lb}{rad}$

$\lambda = .0825$ to $.3195$ [1]

$I_\beta = 40270$ sl-ft^2

$\omega_v = 14.975 \frac{rad}{sec}$

$\omega_w = 10.336 \frac{rad}{sec}$

$\omega_\phi \cong 122.26 \frac{rad}{sec}$

TABLE A2

Station	$\bar{x}$	θ	θ'	$\bar{C}$	$\bar{e}_I$	$\bar{k}_m^2 = \bar{k}_4^2$	$\bar{k}_{m_2}^2 = \bar{k}_{m_1}^2$
1	0.0	.555	-1.386	1.824	-.0022	.000129	0.0
2	.111	.401	-1.359	1.824	-.0030	.000403	.000173
3	.2222	.253	-1.152	1.824	-.0030	.000379	.000233
4	.3333	.145	-.761	1.649	-.0023	.000298	.000209
5	.4444	.084	-.486	1.475	.0005	.000215	.000158
6	.5556	.037	-.351	1.301	.0003	.000161	.000126
7	.6667	.006	-.212	1.131	.0003	.000108	.000090
8	.7778	-.010	-.153	.956	.0003	.000078	.000067
9	.8889	-.028	-.126	.782	.0002	.000074	.000065
10	1.0	-.038	-.090	.608	.0005	.000039	.000039

(rad.)

TABLE A2 Continuted

Station	γ_r	γ_r'	γ_r''	γ_w	γ_w'	γ_w''	γ_ϕ	γ_ϕ'
1	0.0	0.0	2.504	0.0	0.0	.683	.582	.313
2	.017	.293	2.283	.005	.126	1.229	.615	.246
3	.065	.531	1.620	.028	.311	1.571	.641	.292
4	.135	.720	1.473	.074	.482	1.024	.685	.383
5	.225	.945	2.209	.135	.680	1.980	.733	.441
6	.345	1.170	1.473	.225	.959	2.254	.791	.566
7	.485	1.328	1.105	.348	1.260	2.322	.869	.671
8	.640	1.463	1.105	.505	1.719	4.644	.952	.513
9	.810	1.620	1.473	.730	2.228	3.073	.992	.200
10	1.0	1.710	0.0	1.0	2.430	0.0	1.0	0.0

TABLE A2 Continued

Station	$EI_1 \times 10^{-8}$	$EI_2 \times 10^{-8}$	$GJ \times 10^{-8}$	$EB_1 \times 10^{-8}$	$EB_2 \times 10^{-8}$
1	1.19	1.19	.903	4.37	-1.55
2	1.88	2.15	1.32	3.73	-1.43
3	.632	1.21	.472	3.32	-1.35
4	.396	.951	.250	2.16	-.986
5	.257	.771	.153	1.35	-.696
6	.139	.576	.083	.794	-.472
7	.073	.403	.035	.443	-.306
8	.028	.181	.017	.223	-.184
9	.017	.069	.014	.098	-.100
10	.024	.035	.014	.035	-.046
	($lb\text{-}ft^2$)	($lb\text{-}ft^2$)	($lb\text{-}ft^2$)	($lb\text{-}ft^4$)	($lb\text{-}ft^3$)

2B. Equivalent Hinge Model

The parameters defined in Ref. 1 were calculated and are listed in Table A3.

TABLE A3

λ = .0825 nom. to .3195

θ_o = 0

γ = 11.25

$\frac{c_{DO}}{a}$ = .002

$\frac{c}{R_T}$ = .0398

ν_β = 2.572

ν_ϕ = 3.62

ν_θ = 29.19

I_o = .00105

$\beta_S = \beta_H$ = -.12

ϕ_S = 0

χ_A = 0

χ_I = -.00152

α_s = .166

Appendix III

Equivalent Hinge Coefficients

The equivalent hinge matrix coefficients of Ref. 1 are listed here for convenience:

$$M_{11} = 1$$

$$M_{12} = \frac{3}{2} x_I (\beta_o - \beta_H)$$

$$M_{13} = \frac{3}{2} x_I + \phi_o$$

$$M_{21} = \frac{3}{2} x_I (\beta_o - \beta_H)$$

$$M_{22} = 1$$

$$M_{23} = -(\beta_o - \beta_H)$$

$$M_{31} = \frac{3}{2} x_I + \phi_o$$

$$M_{32} = -(\beta_o - \beta_H)$$

$$M_{33} = I_o + (\beta_o - \beta_H)^2 + \phi_o^2 + 3 x_I^2 + 3 \phi_o x_I$$

NOTE: $1 \approx w$

$2 \approx v$

$3 \approx \phi$

$$C_{11} = \frac{\gamma}{8} + 2\eta_\beta \nu_\beta$$

$$C_{12} = 2\beta_o + \frac{\gamma}{6}(\lambda - 2\theta_o)$$

$$C_{13} = -2\beta_o(\beta_o - \beta_H) + \frac{\gamma}{6}\left[-(\beta_o - \beta_H)(\lambda - 2\theta_o) + \frac{3}{4}\phi_o - \left(\frac{c}{2R_T} - x_A\right)\right] - \frac{\gamma}{12}\frac{c}{2R_T}$$

$$C_{21} = -2\beta_o - \frac{\gamma}{6}(2\lambda - \theta_o)$$

$$C_{22} = \frac{\gamma}{4}\left(\frac{c_{Do}}{a} + \lambda\theta_o\right) + 2\eta_\phi \nu_\phi$$

$$C_{23} = -2\beta_o\left(\phi_o + \frac{3}{2}x_I\right) + \frac{\gamma}{4}\left[-(\beta_o - \beta_H)\left(\frac{c_{Do}}{a} + \lambda\theta_o\right) + (2\lambda - \theta_o)\left(\frac{c}{2R_T} - x_A - \frac{2}{3}\phi_o\right)\right] + \frac{\gamma}{8}\lambda\frac{c}{2R_T}$$

$$C_{31} = 2\beta_o(\beta_o - \beta_H) + \frac{\gamma}{6}\left[(\beta_o - \beta_H)(2\lambda - \theta_o) + \frac{3}{4}\phi_o + x_A\right]$$

$$C_{32} = 2\beta_o\left(\phi_o + \frac{3}{2}x_I\right) + \frac{\gamma}{4}\left[-(\beta_o - \beta_H)\left(\frac{c_{Do}}{a} + \lambda\theta_o\right) + \frac{2}{3}(\lambda - 2\theta_o)\left(\phi_o + \frac{3}{2}x_A\right)\right]$$

$$C_{33} = 2\eta_\theta \nu_\theta (I_o + 3x_I^2) + \frac{\gamma}{6}\left[(\beta_o - \beta_H)\left(\phi_o + \frac{3}{2}x_A\right)(\lambda + \theta_2) + \frac{3}{4}\phi_o^2 - \frac{3}{2}(\beta_o - \beta_H)(2\lambda - \theta_o)\frac{c}{2R_T} - \left(\frac{c}{2R_T} - 2x_A\right)\phi_o + \frac{3}{2}x_A\left(\frac{c}{2R_T} - x_A\right) + \frac{3}{2}(\beta_o - \beta_H)^2\left(\frac{c_{Do}}{a} + \lambda\theta\right)\right] - \frac{\gamma}{8}\left[x_A + \lambda(\beta_o - \beta_H) + \frac{2}{3}\phi_o\right]\frac{c}{2R_T} + \frac{\gamma}{8}\left(\frac{c}{2R_T}\right)^2$$

$$K_{11} = 1 - 2\beta_0^2 + \beta_H^2 + \nu_\beta^2 \cos^2\alpha_s + \nu_\phi^2 \sin^2\alpha_s$$

$$K_{12} = -\beta_H\left(\phi_0 + \frac{3}{2}x_I\right) + \frac{\gamma}{8}\beta_H + (\nu_\phi^2 - \nu_\beta^2)\sin\alpha_s\cos\alpha_s$$

$$K_{13} = -\frac{\gamma}{8} + \phi_0 + \frac{3}{2}x_I$$

$$K_{21} = -\beta_H\left(\phi_0 + \frac{3}{2}x_I\right) + \frac{\gamma}{4}x_A(\lambda - \theta_0)$$
$$+ \frac{\gamma}{8}\left[(-3\beta_0 + \beta_H)\frac{C_{D0}}{a} + 2(2\lambda - \theta_0)\left(\frac{c}{2R_T} - x_A\right)\right]$$
$$+ (\nu_\phi^2 - \nu_\beta^2)\sin\alpha_s\cos\alpha_s$$

$$K_{22} = -\beta_H\beta_0 + \nu_\phi^2\cos^2\alpha_s + \nu_\beta^2\sin^2\alpha_s - \frac{\gamma}{6}\beta_H(2\lambda - \theta_0)$$

$$K_{23} = \beta_0 + \frac{\gamma}{6}(2\lambda - \theta_0)$$

$$K_{31} = \phi_0 + \frac{3}{2}x_I - \frac{\gamma}{8}\left(\frac{C_{D0}}{a} + 2\theta_0\lambda - 2\lambda^2\right)$$

$$K_{32} = \beta_0 + \frac{\gamma}{6}(\lambda - \theta_0)$$

$$K_{33} = I_0 - \beta_0(\beta_0 - \beta_H) + \phi_0^2 + 3x_I\phi_0 + 3x_I^2 + I_0\nu_\theta^2$$
$$+ \frac{\gamma}{6}\left[-(\beta_0 - \beta_H)(2\lambda - \theta_2) - \frac{3}{4}\phi_0 - x_A\right]$$

References

1. Miller, R. H., et al., "Wind Energy Conversion," Vol. 1-10, Final Report, M.I.T. ASRL TR 184-7 to TR 184-17, August 1978.

2. Workshop Proceedings: Wind Energy Conversion Systems, NASA TM X-69786, December 1973.

3. Putnam, P. C., Power from the Wind, Van Nostrand Reinhold Company, New York, N.Y., 1948.

4. Spera, D. A., "Structural Analysis of Wind Turbine Rotors for NSF-NASA MOD-0 Wind Power System," NASA TM X-3198, March 1975.

5. Donham, R. E., Schmidt, J., and Linscott, B. S., "100 kw Hingeless Metal Wind Turbine Blade Design, Analysis, and Fabrication," Proceedings of the 31st Annual National Forum of the American Helicopter Society, Washington, D.C., May 1975.

6. Chamis, C. C. and Sullivan, T. L., "Free Vibrations of the ERDA-NASA 100 kw Wind Turbine," NASA TM X-71879, 1976.

7. Hodges, D. H. and Dowell, E. H., "Nonlinear Equations of Motion for the Elastic Bending and Torsion of Twisted Nonuniform Rotor Blades," NASA TN D-7818, December 1974.

8. Hodges, D. H. and Ormiston, R. A., "Stability of Elastic Bending and Torsion of Uniform Cantilever Rotor Blades in Hover with Variable Structural Coupling," NASA TN D-8192, April 1976.

9. Friedmann, P. P., "Recent Developments in Rotary-Wing Aeroelasticity," AIAA Journal of Aircraft, Vol. 14, No. 11, November 1977, pp. 1027-1041.

10. Houbolt, J. C. and Brooks, G. W., "Differential Equations of Combined Flapwise Bending, Chordwise Bending, and Torsion of Twisted, Nonuniform Rotor Blades," NACA Report 1346, 1958.

11. Friedmann, P. P., and Yuan, C., "Effect of Modified Aerodynamic Strip Theories on Rotor Blade Aeroelastic Stability," AIAA Journal, Vol. 15, No. 7, July 1977, pp. 932-940.

12. Bisplinghoff, R. L., Ashley, H., and Halfman, R. L., Aeroelasticity, Addison-Wesley Publishing Co., Inc., Cambridge, Mass., 1955.

13. Greenberg, J. M., "Airfoil in Sinusoidal Motion in a Pulsating Stream," NACA TN 1326, 1947.

14. Miller, R. H. and Ellis, C. W., "Helicopter Blade Vibration and Flutter," Journal of the American Helicopter Society, Vol. 1, No. 3, July 1956.

15. Friedmann, P. P., "Aeroelastic Modeling of Large Wind Turbines," Journal of the American Helicopter Society, October 1976, pp. 17-27.

16. Bramwell, A.R.S., Helicopter Dynamics, John Wiley and Sons, Inc., New York, N.Y., 1976.

17. Mil', et al., "Helicopters: Calculation and Design: Volume I, Aerodynamics", "Mashinostroyeniye" Publishing House, Moscow, 1966, NASA TT F-494, September 1967.

18. Meirovitch, L., Analytical Methods in Vibrations, The MacMillan Company, New York, N.Y. 1967.

19. Loewy R. G., "Review of Rotary-Wing V/STOL Dynamic and Aeroelastic Problems," Journal of the American Helicopter Society, Vol. 14, No. 3, July 1969, pp. 3-23.

20. Friedmann, P. P., "Influence of Modeling and Blade Parameters on the Aeroelastic Stability of a Cantilevered Rotor," AIAA Journal, Vol. 15, No. 2, February 1977, pp. 149-158.

☆ U.S. GOVERNMENT PRINTING OFFICE: 1980-640-258/262